

**MODELING OF NEAR-WELLBORE WETTABILITY
ALTERATION FOR GAS WELL LIQUID BLOCKING
REMEDICATION**

A Thesis

by

BESTRAMY DELFARZA SANTOSO

Submitted to the Office of Graduate and Professional Studies of
Texas A&M University
in partial fulfillment of the requirements for the degree of

MASTER OF SCIENCE

Chair of Committee,
Co-Chair of Committee,
Committee Member,
Head of Department,

Hadi Nasrabadi
Maria Barrufet
Ding Zhu
Dan Hill

December 2015

Major Subject: Petroleum Engineering

Copyright 2015 Bestramy Delfarza Santoso

ABSTRACT

Gas condensate reservoirs are prone to developing condensate blocking. This occurs because of the nature of condensate gas reservoirs, wherein reservoir gases experience retrograde condensation; a phenomenon where gases temporarily turn into liquid due to reduction in pressure. This is most pronounced near the wellbore region due to pressure decrease associated with gas production. Because of the reservoir rock's liquid wetting state, the liquid condensate mobility is severely reduced, blocking both gas and condensates from being produced, and severely reducing the productivity of the well. Several studies, both experimental and simulation work suggests that wettability alteration is a serious option available to mitigate condensate blocking, especially as a long-term solution.

This thesis presents both experimental wettability alteration with a commercial surfactant and modeling work done on a well that has near wellbore wettability altered. The experimental studies will explore the effect of surfactants on rock cores to alter its wettability to intermediate wet. The model will investigate effectiveness of wettability alteration when applied to a well. It will examine the effects of chemical reach on ultimate gas recovery, the impact of multiple treatments, and most importantly, costs associated with such treatments. The results of the study show that increasing treatment reach is beneficial to overall gas recovery, and that multiple treatments still yield better recovery than untreated case. However, the cost of the treatment is prohibitive, and is largely dependent on both treatment chemical cost and the cost of lost production during

treatment. This study illustrates the importance of treatment longevity and the need of low-cost chemicals for well deployment.

DEDICATION

*To my father, who labors to provide me with the best support he can, and to my mother,
who sacrificed her own time to be beside me during the completion of this thesis,*

*To my friends both in Qatar and College Station who keeps me sane, educated, and
motivated: Mohamed “AJ” Abdulsalam, Shubham Agrawal, Manzoor Ahmed, Hesham
Fahmy, Vena Eveline, Tiurma Theresa, Reza Alfajri, Wisnu Nugroho, Gama Firdaus,
and many others,*

*To Dr. Fahes that made this all possible, and to Dr. Nasrabadi who guides me through
to completion,*

To everyone, I can only say one thing:

Thank you. It truly has been an honor.

ACKNOWLEDGEMENTS

I am grateful to my supervisor Dr. Hadi Nasrabadi for his guidance in finishing this thesis. I would also like to thank Dr. Mashhad Fahes for her initial recommendation to this initial research that would lead to the creation of this thesis. I would like to acknowledge Qatar National Research Fund for funding of the research. The equipments, facilities and resources provided by Texas A&M University at Qatar and Texas A&M University in College Station are gratefully acknowledged.

TABLE OF CONTENTS

	Page
ABSTRACT	ii
DEDICATION	iv
ACKNOWLEDGEMENTS	v
TABLE OF CONTENTS	vi
LIST OF FIGURES	viii
LIST OF TABLES	xi
1. INTRODUCTION.....	1
1.1 Research Objectives	3
1.2 Qatar's North Field.....	4
1.3 Reservoir Fluids	5
1.4 Productivity Decline Due to Condensate Buildup	7
1.5 Proposed Methods to Alleviate Condensate Blocking	9
2. THEORETICAL ANALYSIS	14
2.1 Wettability	14
2.2 Surfactants	15
3. EXPERIMENTAL WORK	18
3.1 Experimental Setup and Procedures.....	18
3.2 Rock Preparation	19
3.3 Absolute Permeability and Porosity Measurements.....	20
3.4 Spontaneous Liquid Imbibition	21
3.5 Contact Angle Tests	22
3.6 Chemical Treatment	23
3.7 Treatments with SA05611	24
4. SIMULATION	31
4.1 Equations and Assumptions	31
4.2 Treatment Radius	36
4.3 Water Injection Quantity Simulation	42

4.4 Multiple-Treatment Case.....	47
5. ECONOMIC ANALYSIS	50
5.1 Single-Treatment Case	50
5.2 Multiple-Treatment Case.....	53
5.3 Hypothetical Multiple-Treatment Scenario.....	55
6. CONCLUSION AND RECOMMENDATIONS	57
REFERENCES	59
APPENDIX A	65
APPENDIX B	68
APPENDIX C	72
APPENDIX D	74
APPENDIX E.....	76

LIST OF FIGURES

	Page
Fig. 1 – Productivity index graph of a gas condensate well in Arun field, Indonesia. The decrease is linked to condensate buildup as pressure decreases. (Modified from Afidick, Kaczorowski, and Bette, 1994).....	2
Fig. 2 – Phase diagram of a retrograde gas (Modified from Fan et al. 2005)	5
Fig. 3 – Near-borehole profile in a gas-condensate well showing relative permeabilities of gas and condensate, as well as condensate saturation (modified from Fan et al. 2005)	6
Fig. 4 – Sensitivity to critical condensate saturation (modified from Barnum et al., 1995)	9
Fig. 5 – Contact angle with treated and untreated Berea core (modified from Wu and Firoozabadi, 2010)	11
Fig. 6 – Contact angle	14
Fig. 7 – Surfactant micelle (modified from Evans and Wennerström, 1994)	16
Fig. 8 – Structure of SA05611	18
Fig. 9 – Core preparation tools.....	19
Fig. 10 – Plot of sample ILY30 used for absolute permeability calculation.....	21
Fig. 11 – The setup used for spontaneous liquid imbibition. (a) The setup consists of a scale connected to a data acquisition setup. The core is hanging under the scale while immersed in liquid. (b) The core is wrapped with a nylon thread to support it.....	22
Fig. 12 – Goniometer for static and dynamic contact angle measurement	23
Fig. 13 – Decane saturation vs. time for core ILY21 following Cases 1 and 2	25
Fig. 14 – Contact angles for the water-gas-rock and oil-gas-rock systems after the Case 2 treatment. Water droplet contact angle is 90° while n-Decane contact angle is 80°	26
Fig. 15 – Decane saturation vs. time for rock ILY30 treated at 24°C with 0.36% SA05611, 0.66% NaHCO ₃ , 33% Methanol and 66% Water	27

Fig. 16 – Decane saturation vs. time for rock ILY31 treated at 24°C with 0.44% SA05611, 1.10% NaHCO ₃ , 43.5% Methanol, 44% Water and 11% Ethanol...	27
Fig. 17 – Decane saturation vs. time for rock ILY32 treated at 24°C with 0.49% SA05611, 2.43% NaHCO ₃ , 21.8% Methanol, 68% Water and 7% Ethanol.....	28
Fig. 18 – Decane saturation vs. time for rock ILY33 treated at 24°C with 0.25% SA05611, 1.47% NaHCO ₃ , 27% Methanol, and 71% Water	29
Fig. 19 – Decane saturation vs. time for rock ILY34 treated at 100°C with 0.5% SA05611, 0.5% NaHCO ₃ , 27.2% Methanol, and 71.8% Water	29
Fig. 20 – Intermediate gas wetting relative permeability curve	34
Fig. 21 – Strong liquid wetting relative permeability curve	35
Fig. 22 – Ultimate gas recovery vs treatment radius, 10 md, intermediate gas wetting case	37
Fig. 23 – Ultimate gas recovery vs treatment radius for 1 md, intermediate gas wetting case	38
Fig. 24 – Ultimate gas recovery vs. treatment radius for 100 md, intermediate gas wetting case	39
Fig. 25 – Pressure profile of 100 md model at the end of production run	40
Fig. 26 – Condensate buildup radius for 100 md model at the end of production run.....	41
Fig. 27 – 200 bbl/d water injection on 10 md field model	43
Fig. 28 – 200 bbl/d water injection on 1 md field model	44
Fig. 29 – Water saturation at 16 feet vs. water injection rate for 100 md, intermediate gas case.....	45
Fig. 30 – Water saturation at 30 feet vs. water injection rate for 100 md, intermediate gas case.....	45
Fig. 31 – Water saturation at 60 feet vs. water injection rate for 100 md, intermediate gas case.....	46

Fig. 32 – Ultimate gas recovery for varying treatment intervals, 100md intermediate wet model	48
Fig. 33 – Ultimate gas recoveries of treated against untreated reservoir models for 100md, intermediate gas case.....	49

LIST OF TABLES

	Page
Table 1 – List of chemicals investigated for their role in wettability alteration. (Modified from Kumar, Pope, and Sharma, 2006)	12
Table 2 – Reservoir model properties for simulation.....	33
Table 3 – Gas-condensate fluid composition and parameters	33
Table 4 – Basic assumptions on economic analysis.....	50
Table 5 – Treatment, water, and downtime expenses. The two entries for 100 md models represent 1 foot and 16 feet treatment radii, respectively.	52
Table 6 – Profitability of treatment in 10 md cases	52
Table 7 – Profitability of treatment in 1 md cases	52
Table 8 – Profitability of treatment in 100 md cases	53
Table 9 – Expenses calculation for multiple treatment cases. The Total Cost Terms a and b refers to 1 foot and 16 feet treatment radii, respectively.....	54
Table 10 – Performance for multiple treatment case, 100md reservoir	54
Table 11 – Initial conditions with reduced surfactant price	56
Table 12 – Profitability of hypothetical treatment using low-cost chemical	56

1. INTRODUCTION

Gas production is set to increase in the years to follow. With rapid growth in industries all over the world, demand for natural gas to fuel such growth can be expected to follow. While oil production has and will account for the majority of all produced hydrocarbons, gas production is rapidly following in demand. Several factors contribute to this. New coal and oil reserves are more difficult to locate, and most efforts are currently spent on how to better exploit existing sources. In contrast, gas wells are relatively plentiful, and recent advances in technology such as hydraulic fracturing, opened access to previously untapped resources of gas. Furthermore, gas-to-liquid technology, and cleaner burning by gas compared to oil and coal will ensure that natural gas will be in high demand well into the next half century.

Like oil, natural gas is a nonrenewable source of fuel derived from remains of animals trapped inside sediments for millions of years. Natural gas however, follows a different path than oil. They become gas depending on source material (kerogen), burial depth and temperature; higher temperatures, and usually correspondingly deeper depths generate gas. Despite so, not all gases are created equal; some gases are buried so deep and in environments so hot they are “dry” gases, while some are of other types. While dry gas is primarily composed of methane, condensate gases contain gases with more carbon atoms, which, depending on their constitution, turn into liquids at certain pressure and temperature.

During production of hydrocarbon wells, the pressure of the reservoir tends to dwindle as production is continued, and gas wells are no exception. However, the majority of producing wells produce not just gas or liquid, but a combination of both. In particular, gas condensate wells warrant a special attention; the presence of heavier gas compounds creates situations where, upon reduction of reservoir pressures, the gases will become liquids. When this occurs, liquid banks form near the wellbore, causing relative gas permeability to drop drastically, and thus, causing production to drop drastically. Afidick et al. (1994) reports of a drastic drop in productivity index of a condensate gas well in Arun field, Indonesia (**Fig. 1**).

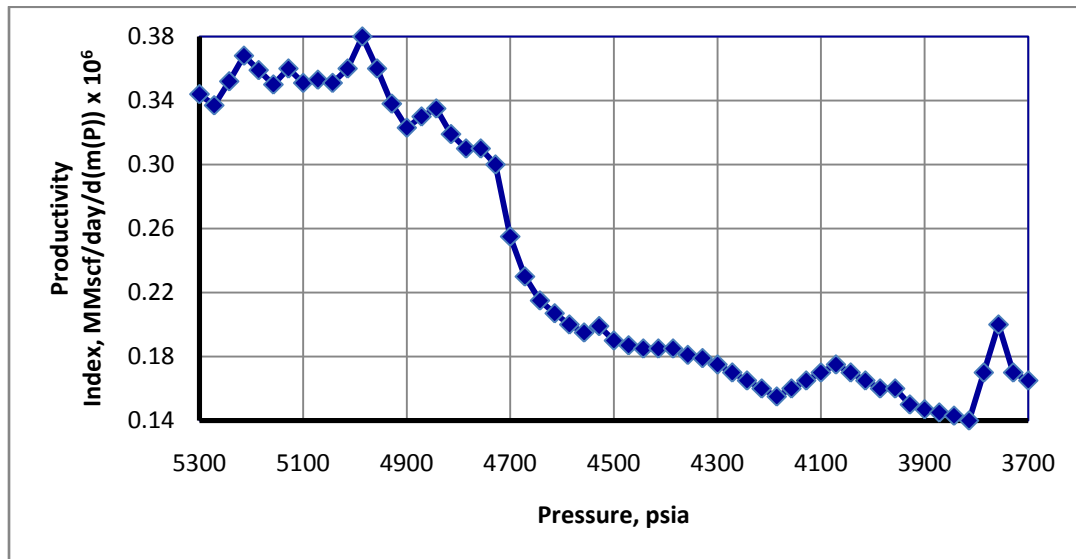


Fig. 1 – Productivity index graph of a gas condensate well in Arun field, Indonesia. The decrease is linked to condensate buildup as pressure decreases. (Modified from Afidick, Kaczorowski, and Bette, 1994)

There are many proposed solutions to the gas condensate blocking problems; anything from gas injection, fracturing, horizontal wells and others have been proposed to counter gas condensate blockage, or at least mitigate it when it occurs. One solution in particular is being advanced as a long term solution in reducing the effect of liquid blocking. That method is the wettability alteration.

1.1 Research Objectives

The objective of this research is to investigate the effect of a wettability alteration treatment on a long term basis on a reservoir. This thesis will focus on both experiments and simulations. The experimental phase will examine the effectiveness of a commercial surfactant on limestone core samples. The simulation phase will focus on three different permeability reservoir models. The objectives are:

- Investigate the effectiveness of altering the wettability of a limestone core using a commercial surfactant.
- Modeling the effect of treatment reach from the wellbore on ultimate gas recovery.
- Modeling the amount of injected water and fluids in order to reach the required radius.
- Examining the implications of a non-lasting effect using multiple treatments.

- Economic analysis of the treatment; taking into account the increase of ultimate recovery contrasted with the price of the chemical and water injections for both single and multiple treatment scenarios.

1.2 Qatar's North Field

Condensate gas fields make up for a large majority of gas wells produced. Despite the inevitable problem of condensate banking, they are more profitable due to condensate sales. There are many fields around the world that produce condensate gases. For example is Indonesia's Arun Field, which contributed to Indonesia's status as the largest exporter of LNG (Liquefied Natural Gas). This continued until 2006, where it was surpassed by Qatar, thanks to large gas production from Qatar's North Field.

Ostensibly a large field, North Field is sometimes also referred to North Field/South Pars Field due to its humongous size and being shared by both Qatar and Iran. The most prolific gas formation is the Permian Khuff field, buried 9,000 feet deep and having a reservoir pressure around 5,300 psia. Divided into noninteracting subsections dubbed K1, K2, K3, and K4, Khuff formations are predominantly made up of crystalline dolomites. The permeability ranges from as low as 0.4 md to 154.4 md. The four subsections have a thickness of 204, 327, 255, and 645 feet, respectively (Whitson and Kuntadi, 2005). The production of gases began with Alpha Project in 1991 after years of quantifying reserves from 1971. The first delivery of LNG began in 1997, and by 2009, at least 7 LNG trains have been built (Benesch et al., 2007).

1.3 Reservoir Fluids

Gas condensates, while not strictly a misnomer, is more accurately referred to as retrograde gas (McCain, 1990). This is due to its retrograde behavior, in which gases condense when its volume is reduced beyond its dew point, but upon further compression, re-evaporates. This is usually encountered on non-pure gases containing multiple compounds, depending on the critical condensation pressure (commonly referred to as *cricondenbar*), and critical condensation temperature (or *cricondentherm*).

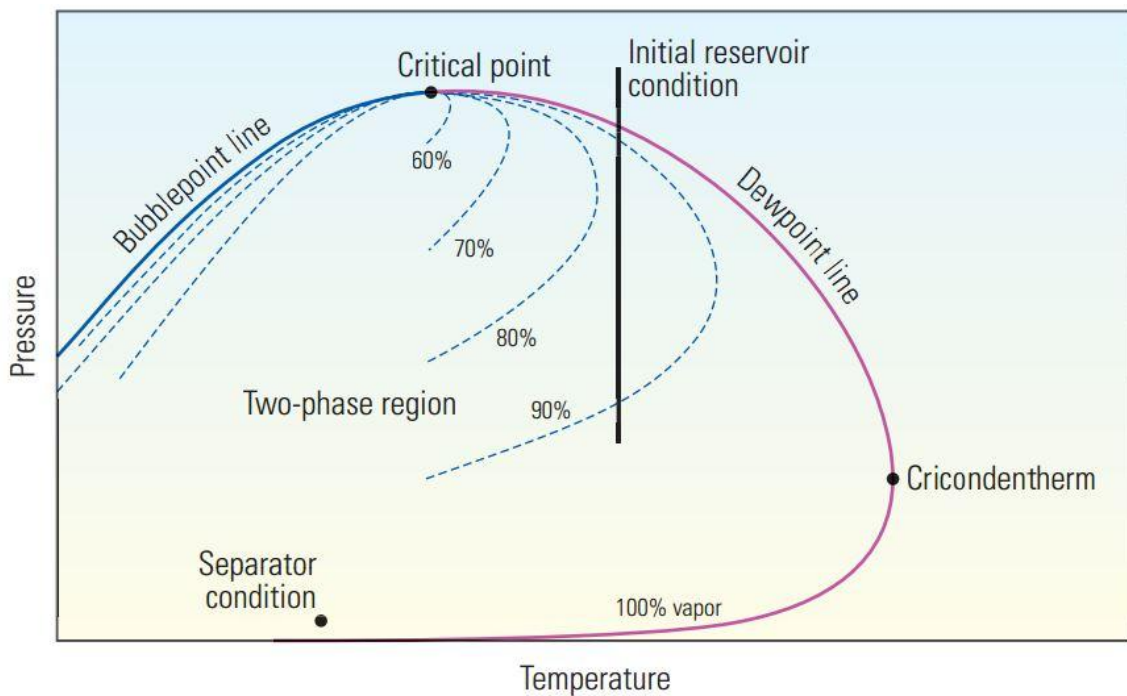


Fig. 2 – Phase diagram of a retrograde gas (Modified from Fan et al. 2005)

From the phase diagram, the area outside the envelope is single phase fluid, either gas or liquid. The area inside the envelope is two-phase, where there is gas and fluid existing at the same time. The bubble point line and dew point line refers to a range of pressures

where liquids start to form gases, and gases start to form liquids, respectively. As delineated by the line in **Fig. 2**, the reservoir gases are most often found as single-phase fluids in reservoir condition, marked with number 1. However, as pressure drops, the gas condenses into liquid. Although the liquids will turn back into gases at even lower pressures, by this point, the liquids are most likely already inside surface facilities.

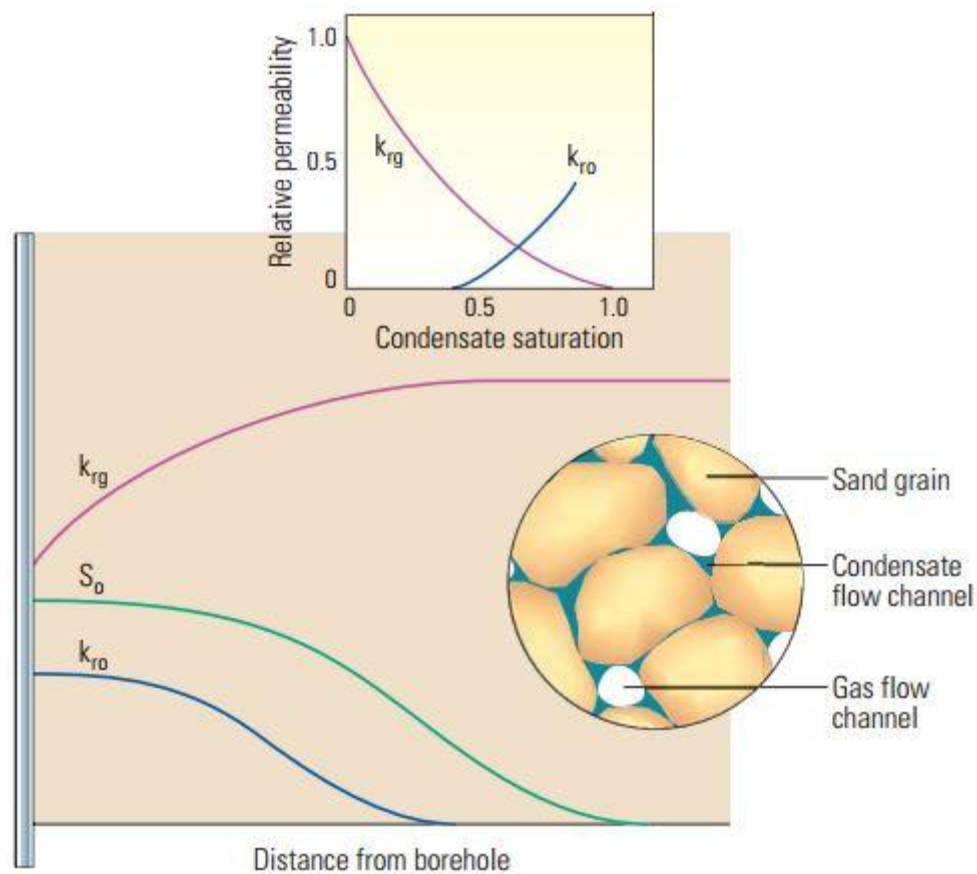


Fig. 3 – Near-borehole profile in a gas-condensate well showing relative permeabilities of gas and condensate, as well as condensate saturation (modified from Fan et al. 2005)

The change from gas to liquid occurs when pressure declines beyond the dew point. While this can theoretically occur across the reservoir at a certain point after a long production run, the more immediate cause occurs near the proximity of the wellbore, as shown by liquid dropout region in the figure above. This liquid buildup near the wellbore causes significant production problems. Assuming an absence of heterogeneities or fractures, the liquids that form near the wellbore would build up continuously. Over time, this buildup would extend farther and farther into the reservoir. The liquids in this region are immobile for most part, and become a significant skin factor that hinders the flow of gas.

1.4 Productivity Decline Due to Condensate Buildup

Condensate buildup near the wellbore has been a major obstacle in sustaining productions for condensate gas wells. Furthermore, the problem almost seems to be inevitable, especially with wells with long production runs. Afidick (1994) reported extensively on the decline of the Arun field in Indonesia, 10 years into production. A 50% drop caused by only 1.1% liquid dropout has been confirmed via phase behavior analysis. On the other hand, the report also noted that even with the liquid dropout, the gas relative permeability was largely unaffected. The results explicitly point to liquid blockage as the cause for production decline.

Another case is the Cal Canal in California, as reported by Engineer (1985). A tight sand formation with permeabilities less than 0.1 md, it produced a rich gas condensate at 280 bbl/MSCF. Production performance history of the field predicts an ultimate recovery no more than 10% at the time of the paper's writing. Reduction of relative permeability due to liquid blockage stemming from condensate buildup is the most likely explanation for this.

Others include Smits et al. (2001) that mentioned two wells by Petroleum Development Oman with production reduction by more than 60% due to condensate buildup, and the paper details efforts to accurately model the buildup. Similarly, studies run by Barnum (1995) have concluded that for permeability-thickness values below 1000 md-ft, gas recovery falls very sharply, especially with higher condensate-to-gas ratio.

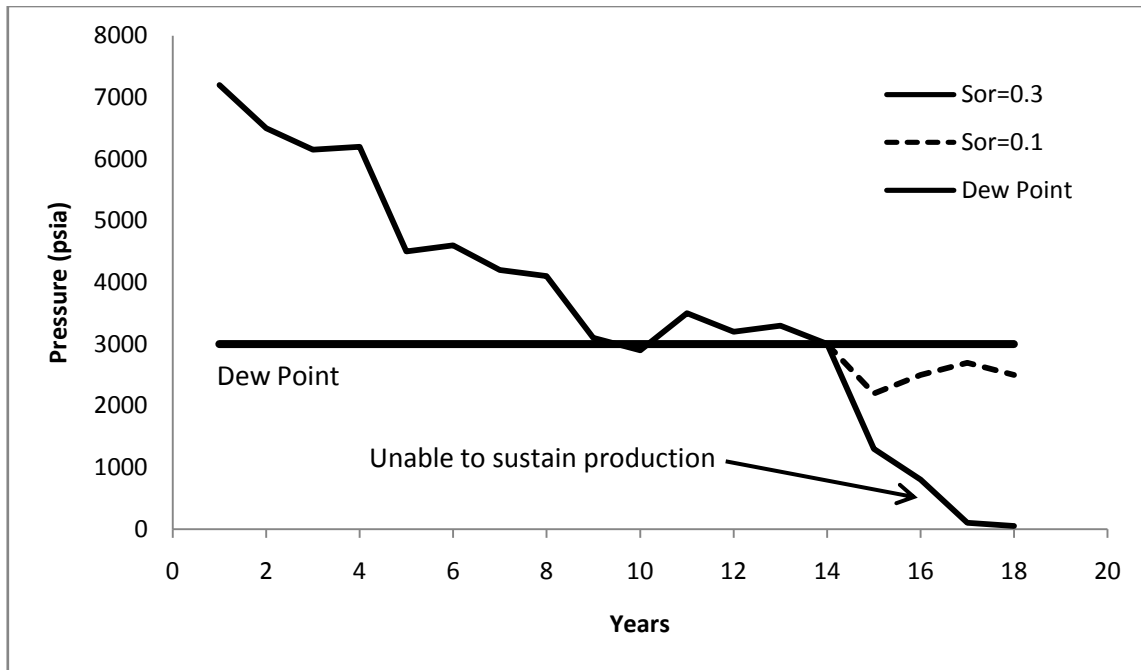


Fig. 4 – Sensitivity to critical condensate saturation (modified from Barnum et al., 1995)

1.5 Proposed Methods to Alleviate Condensate Blocking

Several methods of solutions were proposed to solve the problem of condensate blocking. The most basic solution is reservoir pressure maintenance, thus preventing the pressure to dip below the dew point pressure. These can be achieved through water injection, for example. Other solutions include chemical treatments such as methanol flush treatment (Anazi et al. 2005), “Huff and puff” methods using methane (Jamaluddin et al. 2001) or a combination of lean gas, nitrogen and carbon dioxide (Ahmed et al. 1998), and

hydraulic fracturing (Mohan et al. 2006). However, wettability alteration is touted to be a more permanent and potentially more economic solution.

Surfactants have been used in many aspects of petroleum engineering over the years, especially in the field of enhanced oil recovery. Chukwudeme and Abeysinghe (2014) described their use in minimizing interfacial tension in oil-water systems. One particular use for surfactants is for wettability alteration for condensate banking (Noh and Firoozabadi, 2008; Tang and Firoozabadi, 2002). The use of surfactants requires that it adsorb to pore surfaces, potentially reducing reservoir permeability. Despite so, Mahadevan and Sharma (2005) reported low permeability reduction, at least on laboratory tests. Xu et al.'s paper (2008) has shown that intermediate wet condition has a greater effect than decrease in interfacial tension to alleviate condensate banking. This is further reinforced by Wu and Firoozabadi (2011) that reported an increase of relative permeability of fluids when intermediate wet conditions are achieved, thus also increasing fluid mobility.

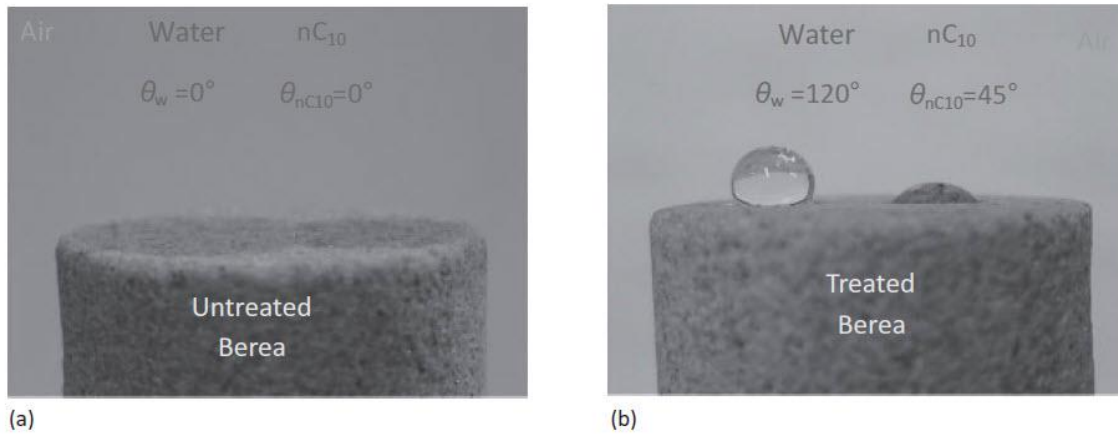


Fig. 5 – Contact angle with treated and untreated Berea core (modified from Wu and Firoozabadi, 2010)

Fluorosurfactants have been recommended for their strong affinity to bind to rock matrices, as well as effectiveness in shifting the wettability to intermediate state, as detailed by Kumar et al. (2008) and Bang et al. (2010). In one example, Fernandez et al. (2011) succeeded in altering the wettability of sandstone rocks utilizing a commercial polytetrafluoroethylene compound named Zonyl. In other papers, Ahmadi et al. (2010) utilized XPS to detect fluorine within surfactants as a selection process to choose surfactants for this purpose.

In other EOR processes such as polymer flood operations, adsorption to rock pores is cited as a potential cause for permeability reduction (Hirasaki and Pope, 1974). In surfactant-induced wettability alteration treatment, adsorption to rock pores is an essential part of the treatment, and thus, the risk of permeability reduction is difficult to

avoid. Fahes and Firoozabadi (2007) determined that chemical makeup of surfactants is a strong factor in determining adsorption. Furthermore, surface charge inside the pores also affects adsorption. Wu and Firoozabadi (2010) concluded that when a rock surface is saturated in brine, chemical adsorption is often affected negatively.

Commercial name	Fluorolink S10	Fluorosyl	Zonyl FSO	Novec FC4430	Novec FC4432
Vendor	Solvey-Solexis	Cytonix	Dupont	3M	3M
Scientific name	Perfluoropolyether ethoxysilane	Perfluorooctal trimethoxysilane	Ethoxylated alkylfluoro-surfactant	Fluoroaliphatic polymeric ester	100% fluoroaliphatic polymeric ester
Chemistry	Silanol	Silanol	Alkoxy	Alkoxy	Alkoxy
Molecular weight	1850	2000	725	~10000	~10000
Specific gravity	1.5	1.4	1.3	1.14	1.21
Boiling point (°C)	N/A	52	N/A	200	212
Viscosity at room temperature (cP)	173	1	5	4000-6000	4000-6001

Table 1 – List of chemicals investigated for their role in wettability alteration.

(Modified from Kumar, Pope, and Sharma, 2006)

Certain chemical properties such as surfactant concentration and molecular weight also affect adsorption (Trogus et al., 1977). While anionic surfactants have been advocated from papers above, specific reservoir conditions may require different surfactants. For example, Sharma and Mohanty (2013) utilizes cationic surfactant with nonionic cosurfactant for high salinity, high temperature condition. Rao et al. (2006) states that anionic surfactant will negatively affect hydrocarbon wet reservoirs, and best avoided for those cases. According to Butler et al. (2009), Trueblood Resources conducted an initial test of surfactant-induced wettability alteration treatment to alleviate condensate

banking. The paper reported a post-treatment increase of four times the gas production, as well as significant condensate gas production, illustrating the potential for this treatment.

2. THEORETICAL ANALYSIS

2.1 Wettability

Wettability is a measure of preference of any solid material to either liquid to gas. It is a function of capillary pressure and surface/interfacial tension, as given by the Young-Laplace equation (Tang and Firoozabadi, 2002),

$$p_c = \frac{2 \cdot \sigma \cdot \cos \theta}{r} \quad (2.1)$$

where p_c is capillary pressure, γ is the interfacial tension, θ being the contact angle, and r being the pore throat radius. Interfacial tension is a force existing in the boundary between two immiscible fluids, such as water and oil or water and gas. When the wettability of a porous media is strongly water wet, interfacial tension and thus capillary pressure is higher. Due to this, immiscible fluid flow through the aforementioned media is drastically reduced. If the interfacial tension of the fluid can be lowered, capillary pressure will be reduced and hence, fluid flow for both types of fluids is less inhibited.

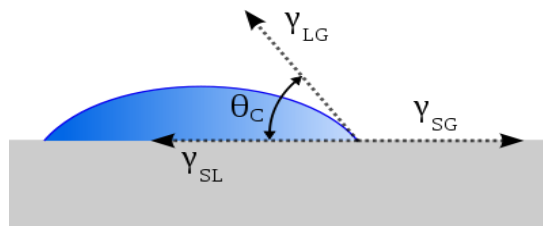


Fig. 6 – Contact angle

The contact angle, or wetting angle, is a thermodynamic variable that depends on interfacial tensions of the material. In the example above, the interfacial tensions are liquid and solid, liquid and gas, and gas and solid. The simplest way to reflect the wettability of the solid phase is through the contact angle; if the contact angle θ_c is 0 degrees, then the solid phase is said to be perfectly liquid-wet. Conversely, a 180 degree θ_c is considered perfectly gas wet.

Tang and Firoozabadi (2002) stated that for gas phase, strong liquid-wet porous media can hold high liquid saturation because of the low mobility of the wetting phase. The aim for wettability alteration is to achieve neither liquid wet nor purely gas wet, but an intermediate wetting one. Thus, when intermediate wetting has been achieved, liquid mobility improves, and thus allows both gas and condensate to be produced, allowing the production to proceed.

2.2 Surfactants

Interfacial tension can be lowered using surfactants that are injected and adsorbed onto the rock pores. Surfactants are chemicals that possess two ends with opposite properties; hydrophilic and hydrophobic. The different properties are useful in many applications such as detergents, where non-water compounds are separated from water by virtue of the hydrophobic ends.

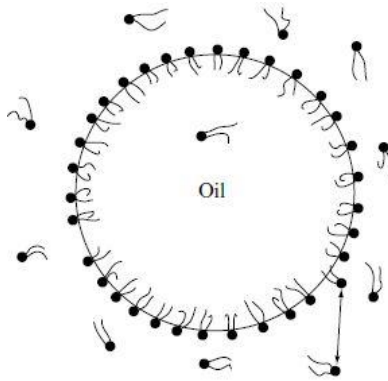


Fig. 7 – Surfactant micelle (modified from Evans and Wennerström, 1994)

At low concentrations, surfactants are similar to electrolytes. As the concentration increases, self-assembly occurs, and surfactants form aggregates called a micelle. Hence, the concentration at which micelles first form is usually referred to as Critical Micelle Concentration, or CMC (Holmberg et al., 2002). The formation of micelles is critical for the alteration of wettability to occur. The CMC is influenced by many factors, including chemical makeup of the surfactant, temperature, and co-solutes. On the other hand, CMC is not affected by pressure. Co-solutes such as salts and alcohols lower the required CMC such that only low concentrations are required for micelles to form; in other words, for the surfactant to be effective.

Surfactants in this case are used to lower interfacial tension in the rock. The adsorption of the surfactants alters the wettability properties of the rock. Changes in the wettability of the rock system will also affect the distribution of fluids in the pore space. When the wettability of the rock matrix reaches an intermediate wet, it lowers the critical

saturation required for condensate to be mobile and hence, allows for both production of gas and condensate.

3. EXPERIMENTAL WORK

3.1 Experimental Setup and Procedures

Through collaboration with Texas A&M at Qatar Wettability Research Group headed by Dr. Mashhad Fahes, several experiments were undertaken to investigate the effect of different surfactants on rock cores. For the purposes of this thesis, the properties of the surfactant chemical are based on a surfactant proposed by Dr. Fahes' team, referred to as SA05611.

SA05611 is a commercial chemical sold by Sigma-Aldrich. The structure of SA05611 is shown in **Fig. 8**. It has a molecular weight of 492.13 g/mol, costing \$200 for 1 gram. It was used in concentrations of 0.2 to 0.7%. The solvents that were used consist of differing proportions of distilled water, methanol, ethanol and isopropyl alcohol. Sodium bicarbonate, NaHCO_3 , was also added to the mixture to help deionise the surfactant in preparation for the adsorption stage.

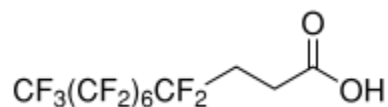


Fig. 8 – Structure of SA05611

According to Wu and Firoozabadi (2010), normal decane (nC_{10}) is considered an adequate stand-in for condensate liquids in terms of wettability alteration study. The gas

phase will be represented by normal air during imbibition tests and nitrogen gas in single and two-phase flow experiments. For comparison, distilled water is used during contact angle tests.

3.2 Rock Preparation

Indiana Limestone samples were cored at Texas A&M University at Qatar. A 1” inner diameter diamond core bit (**Fig. 9a**) and a saw (**Fig. 9b**) was used to cut the core to the desired length.



(a) Drill

(b) Saw.

Fig. 9 – Core preparation tools

The drill and saw use tap water as a coolant during cutting operations. The cores are then placed in the oven for drying at a temperature between 120°C and 140°C. The length,

diameter, and weight of dry rock samples were then measured. Absolute permeability and porosity for the dry rock are then measured at room temperature.

3.3 Absolute Permeability and Porosity Measurements

The absolute permeability is measured using nitrogen single phase flow. In order to conduct this experiment, the rock is packed inside a core holder with an overburden pressure of 1500 psig. A back pressure of over 60 psig is used at the outlet of the rock to eliminate gas-slippage effect. Nitrogen is injected at an inlet pressure between 120 and 150 psig. Back pressure is then set at around 60 psig and the gas standard-condition volumetric flow rate is measured. Back pressure is then increased incrementally and around eight data points are collected. Due to the low permeability of the rock samples, it was observed that Darcy law leads accurate measurements of permeability. The equation that was applied, using Darcy unit system, is the following:

$$\frac{q}{A} = \frac{k}{\mu} \frac{P_1^2 - P_2^2}{2L} \quad (3.1)$$

A plot of $\frac{q}{A}$ vs. $\frac{P_1^2 - P_2^2}{2L}$ is generated as shown in **Fig. 10**. Absolute permeability is then calculated from the slope of the line using a nitrogen viscosity of 0.01787 cp.

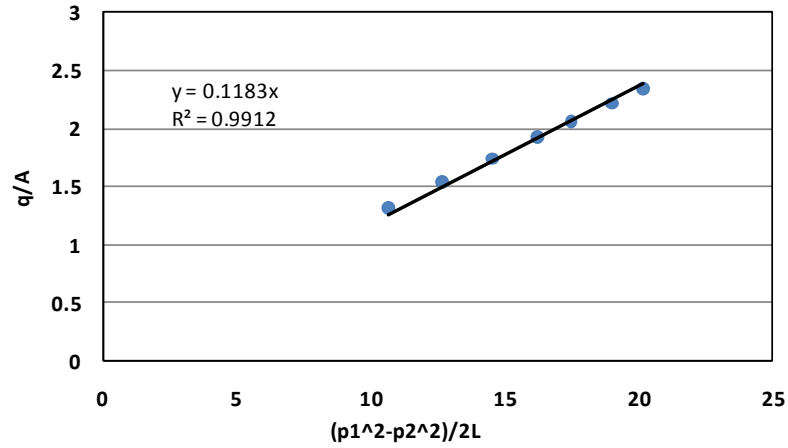


Fig. 10 – Plot of sample ILY30 used for absolute permeability calculation

The porosity of the core samples is measured using a helium porosimeter. Helium is widely used for porosity measurements because it is an inert gas that has low absorption and high diffusivity. The measurements are based on isothermal ideal gas expansion. Pressure readings are taken before and after gas expansion into the pores of the rock and then the volume of the pore space is calculated. Calibrated spacers are used to reduce dead volume in the sample cylinder. Porosity is then calculated using the following equation:

$$\phi = \frac{V_p}{V_b} \quad (3.2)$$

3.4 Spontaneous Liquid Imbibition

The aim of this experiment is to observe the strength of capillary forces in the rock for the liquid-gas system by measuring the rate of liquid imbibition. The dry rock is

wrapped with a nylon thread for support and placed in a liquid-filled beaker (**Fig. 11a**) while hanging under an electronic balance (**Fig. 11b**). The balance is connected to data acquisition system that records the weight of the rock with time. The liquid saturation in the rock with time is then calculated and plotted vs. imbibition time.

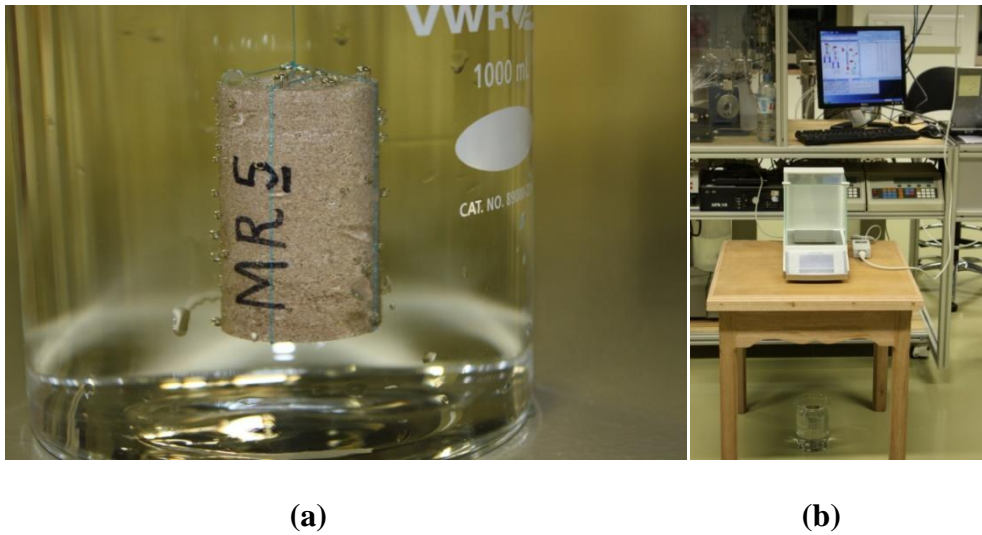


Fig. 11 – The setup used for spontaneous liquid imbibition. (a) The setup consists of a scale connected to a data acquisition setup. The core is hanging under the scale while immersed in liquid. (b) The core is wrapped with a nylon thread to support it

3.5 Contact Angle Tests

A liquid droplet is placed on the surface of the rock and the contact angle is visually estimated. Photos are taken at small time intervals. An example of the contact angle measurement is shown in **Fig. 14**. A goniometer (**Fig. 12**) was used for systematic

measurements of static and dynamic contact angle. The use of the goniometer is to carefully study the effect of chemical concentration on wettability for successful treatments.



Fig. 12 – Goniometer for static and dynamic contact angle measurement

3.6 Chemical Treatment

Wettability alteration is performed by injecting the chemical mixture in liquid form into the rock sample. The mixture carries with it a given concentration of the surfactant being used. The solvent used is water, methanol, isopropyl alcohol, or a mixture of the various solvents. The chemical mixture is placed in a piston accumulator and injected at a constant rate into the rock sample with the aid of a positive displacement pump. In most of the experiments, the rock is initially in a dry state. The rock is placed in the core-holder and an overburden pressure of around 1500 psi is applied before chemical injection starts. The injection rate of the surfactant varies from 0.5 cc/min to around 2

cc/min depending on the length and the permeability of the rock sample keeping the total pressure across the sample below 300 psi. When the treatment is conducted at 24°C, the initial pressure is atmospheric and the outlet pressure during chemical injection is also atmospheric. When the treatment is conducted at 100°C, an initial pressure of 200 psi is established in the rock using nitrogen. The pressure is maintained higher than 200 psi throughout the chemical injection process as well as the aging and displacement steps to prevent solvent evaporation. After a given aging time which varies between 3 and 15 hours, the excess surfactant mixture is displaced from the rock using air, water, methanol, or a combination of the three. The rock is then dried in the oven and various post-treatment measurements are conducted.

3.7 Treatments with SA05611

In Case 1, an Indiana Limestone core ILY21 was treated at 100°C by injecting a mixture of 0.5% SA05611 in a 94% methanol and 5.5% distilled water. A reduction in permeability was noted from 4.5 to 3.8 md (15%). There was no significant difference in the imbibition rate compared to an untreated rock.

In Case 2, the same rock was treated with a mixture of 0.76% SA05611, 0.76% NaHCO₃, 18% Methanol, 74.4% Water and 6% Ethanol to the solution to enhance the mixing of the solution. This treatment was conducted at room temperature. The result was very impressive; the decane imbibition experiment presented in **Fig. 13** shows that oil imbibition almost completely ceased. The contact angle measured was around 80° as

shown in **Fig. 14**, as opposed to 90% with water. The only problem was a reduction in the permeability of the rock from 3.8 to 2.3 md (39%).

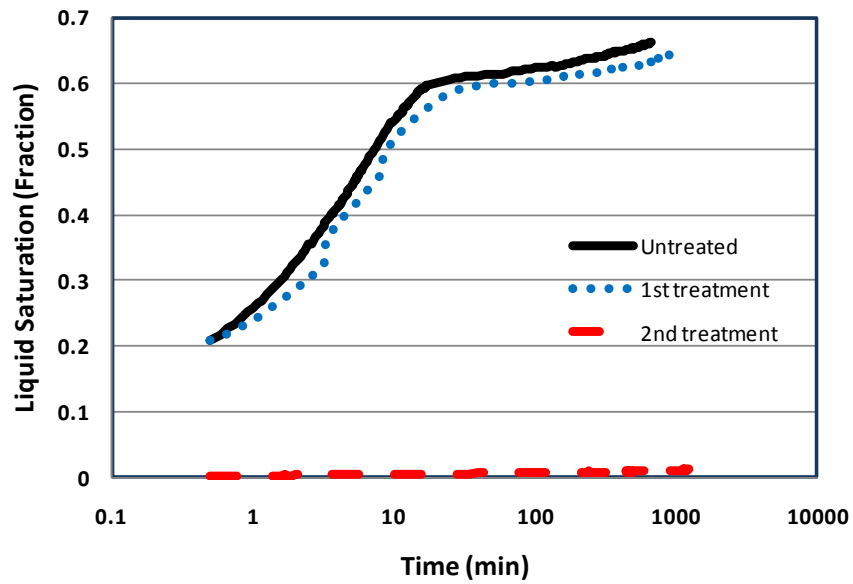


Fig. 13 – Decane saturation vs. time for core ILY21 following Cases 1 and 2

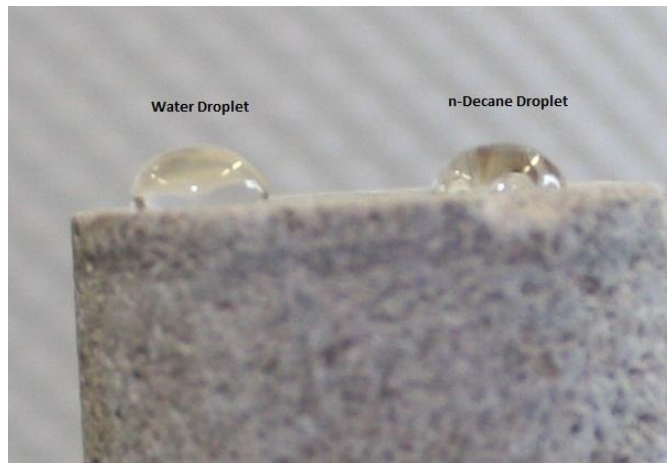


Fig. 14 – Contact angles for the water-gas-rock and oil-gas-rock systems after the Case 2 treatment. Water droplet contact angle is 90° while n-Decane contact angle is 80°

In Case 3, the chemical concentration was reduced. A different rock core (ILY30) was treated with 0.36% SA05611, 0.66% NaHCO_3 , 33% Methanol and 66% Water. The imbibition rate presented in **Fig. 15** reflects a lack of change from untreated sample and the treatment was deemed failure. Curiously, the permeability of the rock did not change. In order to examine whether the absence of Ethanol in the treatment mixture was the reason for the ineffective adsorption, 11% Ethanol was added to the mixture and administered to core ILY31 as Case 4. The result presented in **Fig. 16** shows the treatment was not effective. The concentrations were further altered with a lower concentration of methanol and ethanol, and almost 70% water, but also this treatment was not effective as shown in **Fig. 17**.

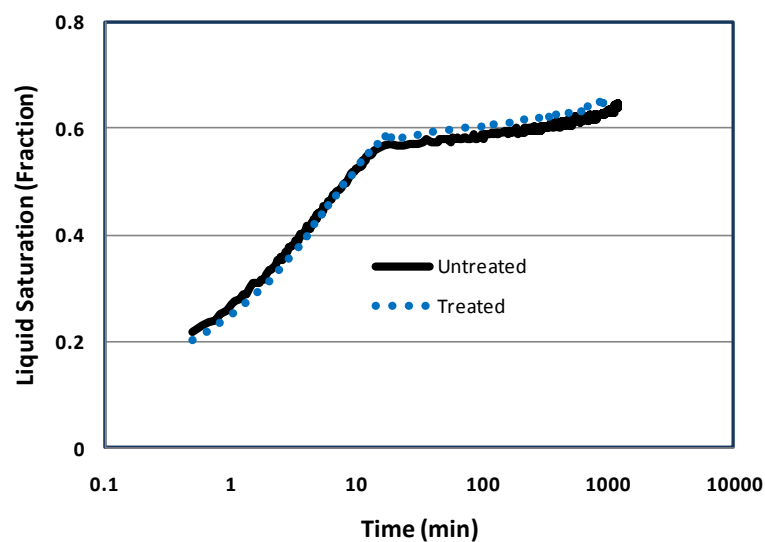


Fig. 15 – Decane saturation vs. time for rock ILY30 treated at 24°C with 0.36% SA05611, 0.66% NaHCO₃, 33% Methanol and 66% Water

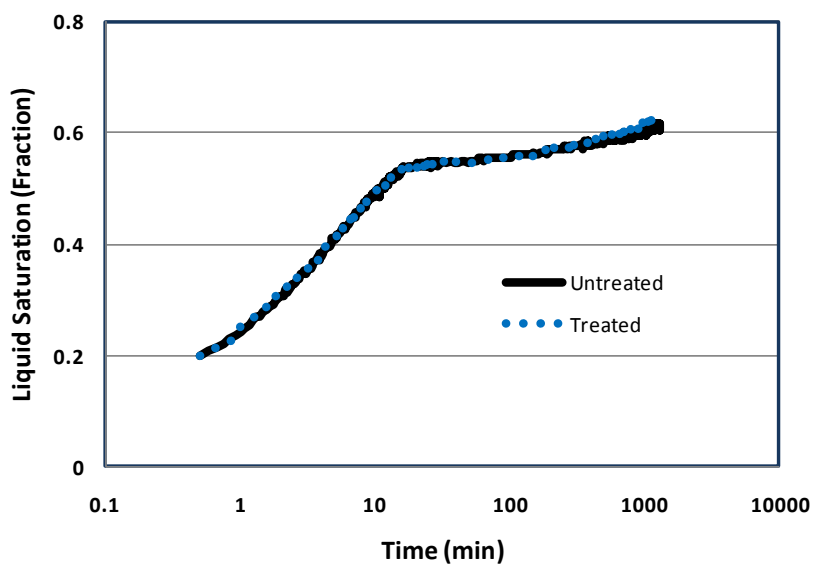


Fig. 16 – Decane saturation vs. time for rock ILY31 treated at 24°C with 0.44% SA05611, 1.10% NaHCO₃, 43.5% Methanol, 44% Water and 11% Ethanol

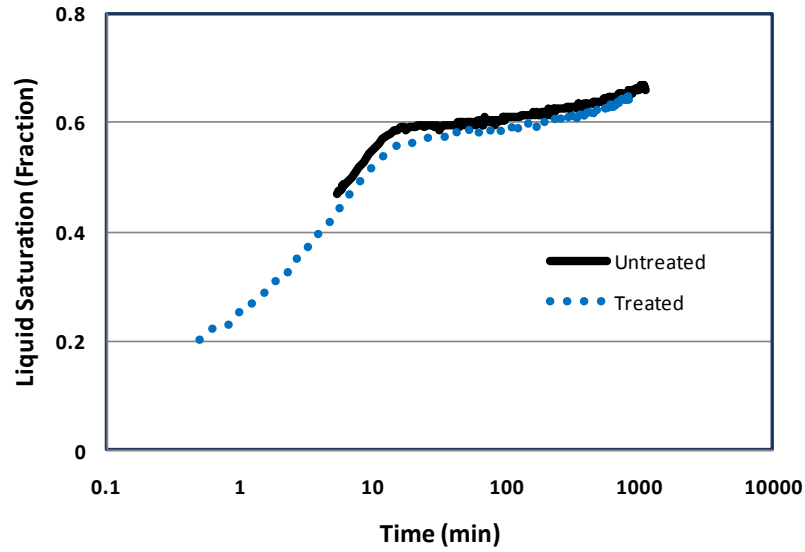


Fig. 17 – Decane saturation vs. time for rock ILY32 treated at 24°C with 0.49% SA05611, 2.43% NaHCO₃, 21.8% Methanol, 68% Water and 7% Ethanol

Based on previous results, the next treatment was planned for ILY33 (case 6) with 0.25% SA05611, 1.47% NaHCO₃, 27% methanol and 71% water. The treatment was conducted at room temperature. It did result in a significant change in the value of the decane imbibition rate as shown in **Fig. 18**, although less than that of ILY21 (Case 2). The permeability was measured to be 2.9 md before treatment and 2.5 md after treatment indicating a reduction of around 14%.

In order to compare the performance of room temperature treatment to that of high temperature treatment, ILY34 (case 7) was treated at 100°C with 0.5% SA05611, 0.5% NaHCO₃, 27.2% methanol and 71.8% water. The results of the imbibition experiment

shown in **Fig. 19** indicate a similar trend to that observed after room temperature treatment. The permeability was also compromised from 2.1 to 1.7, indicating around 19% reduction.

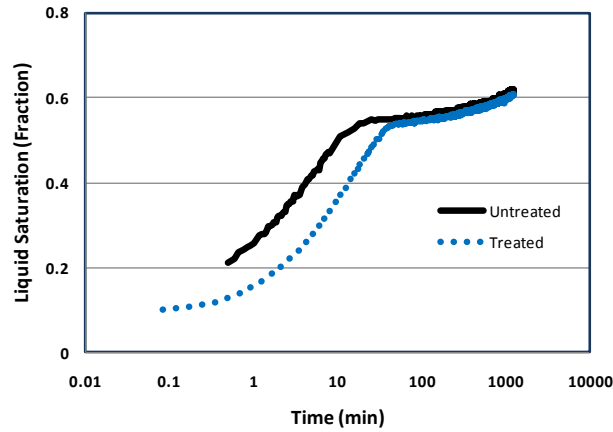


Fig. 18 – Decane saturation vs. time for rock ILY33 treated at 24°C with 0.25% SA05611, 1.47% NaHCO₃, 27% Methanol, and 71% Water

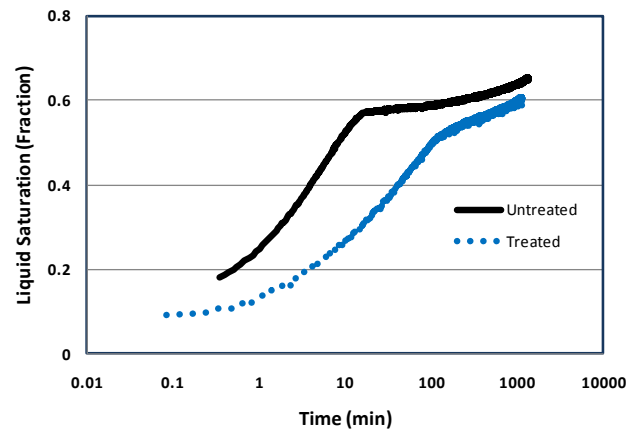


Fig. 19 – Decane saturation vs. time for rock ILY34 treated at 100°C with 0.5% SA05611, 0.5% NaHCO₃, 27.2% Methanol, and 71.8% Water

Despite implementing varying solvent mixtures, further tests that were conducted did not result in any significant alteration of rock wettability. It was proven however, that the surfactant itself under right conditions can affect rock wettability greatly. The next section of this thesis will deal with modelling the effectiveness of the surfactant had a suitable solvent formulation been developed for it.

4. SIMULATION

4.1 Equations and Assumptions

The basis for this simulation work was done by Zoghbi et al. in 2010. In the paper prepared, Zoghbi et al. uses wettability alteration as the treatment to condensate blockage in near-wellbore environment. In it, Zoghbi et al. argued that the design of the treatment must emphasize the gas end-point relative permeability in order for the treatment to be successful. Hence, the simulations done in this thesis will depart from the same assumptions and using modified models employed by Zoghbi et al.

The treatment modeled in this simulation represents the wettability states that occur in the reservoir. The first is liquid wet, representing the state of preferential wetting towards the condensates, with gas endpoint relative permeability of 0.3 and liquid saturation of 50%. At this state, the condensates are fully blocking the wellbore region due to their low mobility. The second state is intermediate wet, with liquid saturation of 30% and gas relative permeability of 0.5. According to Zoghbi et al. and Fahes and Firoozabadi (2007), the intermediate wetting state is the most advantageous state, and is the goal of wettability alteration treatment.

Darcy's Law is a useful tool in modeling near-wellbore flow; one-dimensional version of Darcy's Law calculates effective permeability k_g from volumetric flow rate q_g , with A being the cross-sectional area (assuming a cylindrical core), $P_{i,2}$ being the pressures at inlet and outlet, μ_g being gas viscosity, and L being the length of the core.

$$\frac{q_g}{A} = \frac{k_g}{\mu_g} \frac{(P_2 - P_1)}{L} \quad (5.1)$$

The ratio of effective permeability of gas k_g over absolute permeability of the porous media k_{abs} defines gas relative permeability k_{rg} . Similarly, water relative permeability k_{rw} can be defined in a similar way.

$$k_{rg} = \frac{k_g}{k_{abs}} \quad (5.2)$$

The relative permeability curves for the wettability alteration uses the Corey correlation, which is a power law in water saturation S_w . For a normalized water saturation value,

$$S_{wn} = \frac{S_w - S_{wi}}{1 - S_{wi} - S_{orw}} \quad (4.3)$$

we can then determine the relative permeabilities of both oil and gas. In this scenario, oil is a stand-in for condensate liquid.

$$K_{rg} = k_{rg}^{max} \left(\frac{S_g - S_{gi}}{1 - S_{gi} - S_{oi}} \right)^{n_g} \quad (4.4)$$

$$K_{ro} = k_{ro}^{max} \left(\frac{S_o - S_{oi}}{1 - S_{oi} - S_{gi}} \right)^{n_o} \quad (4.5)$$

In addition, the exponents n_g and n_o required to generate the relative permeability curves are 2 and 4, respectively.

The reservoir modeled in the simulation is a one layered reservoir with uniform absolute permeability. Three permeability values were investigated: 1, 10, and 100 md. The top of the field model has a depth of 8000 feet, and its thickness is 70 feet. For calculation and simulation purposes, the rest of the reservoir was considered to be liquid wet, while the

immediate area around the wellbore are considered to have been treated with intermediate wet conditions having taken place. Table 2 lists the reservoir properties used in the simulation model.

Reservoir Properties	
Average Porosity (%)	12
Absolute Permeability (md)	1, 10, 100
Initial reservoir pressure (psia)	5500
Formation thickness (ft)	70
Well radius (ft)	0.33
Rock compressibility (1/psi)	1×10^{-6}
Reservoir Temperature (F)	220
Depth to Top of Formation (ft)	8000
Dewpoint pressure (psia)	3380

Table 2 – Reservoir model properties for simulation

For simulation purposes, the gas condensate properties will be based on synthetic condensate gas parameters in **Table 3** proposed by Zoghbi et al.

z (g/mol)	% moles	MW	P_c (psia)	T_c (°R)	Acentric Factors	Parachors	Z_c
C ₁ +N ₂	67.93	16.385	662.493	339.66	0.0089	40.9	0.28822
C ₂ +CO ₂	9.9	31.774	740.088	549.54	0.1135	89	0.25749
C ₃	5.91	44.097	615.76	665.69	0.152	150.3	0.2763
C ₄ +C ₅	7.86	62.925	523.322	781.02	0.2029	183.1	0.27438
C ₆	1.81	86	477.03	913.5	0.2637	250.1	0.27346
C ₇ to C ₁₂	5.18	119.02	396.202	1056.06	0.3346	341.9	0.26465
C ₁₃ +	1.41	217.12	283.631	1312.74	0.5972	586.2	0.2598

Table 3 – Gas-condensate fluid composition and parameters

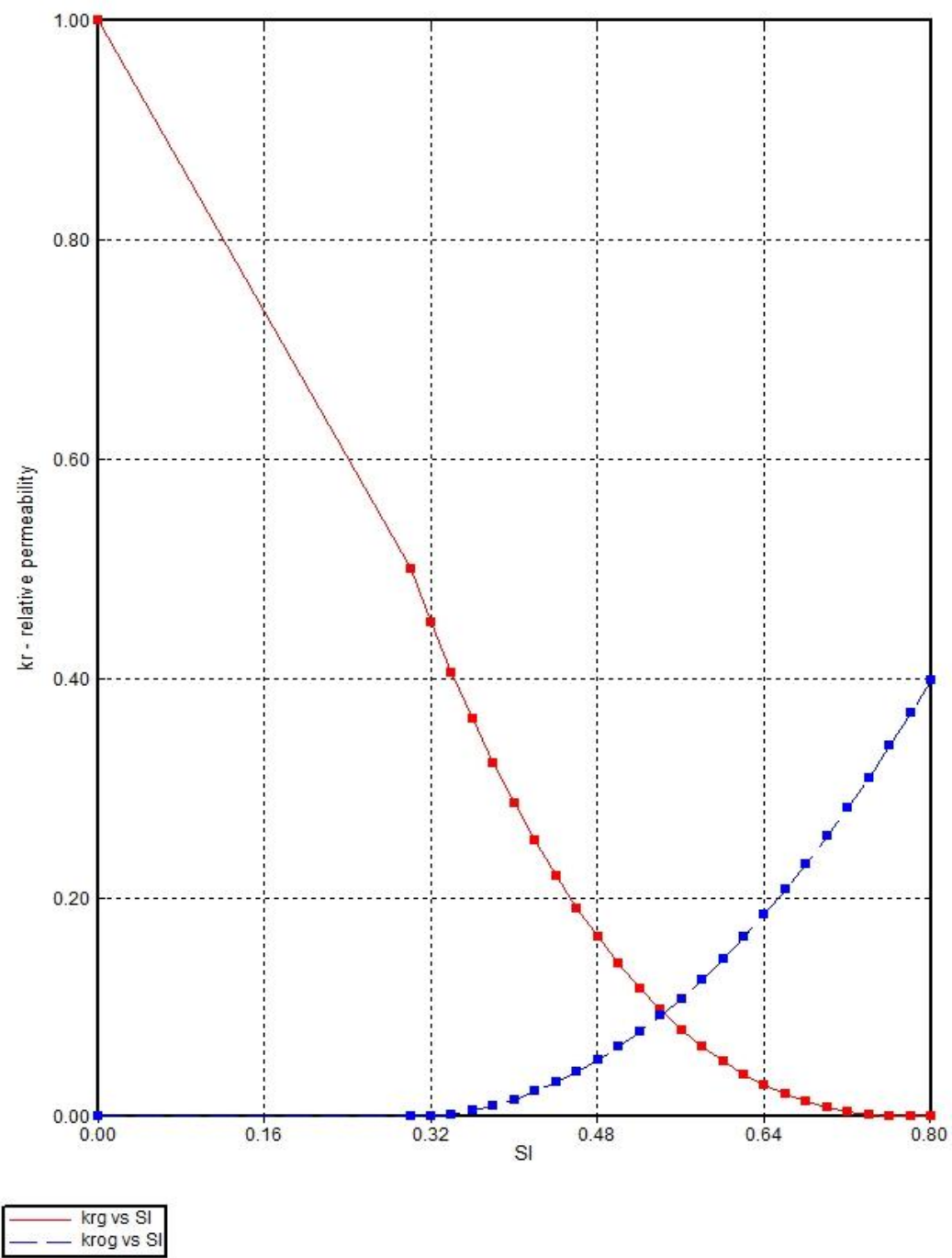


Fig. 20 – Intermediate gas wetting relative permeability curve

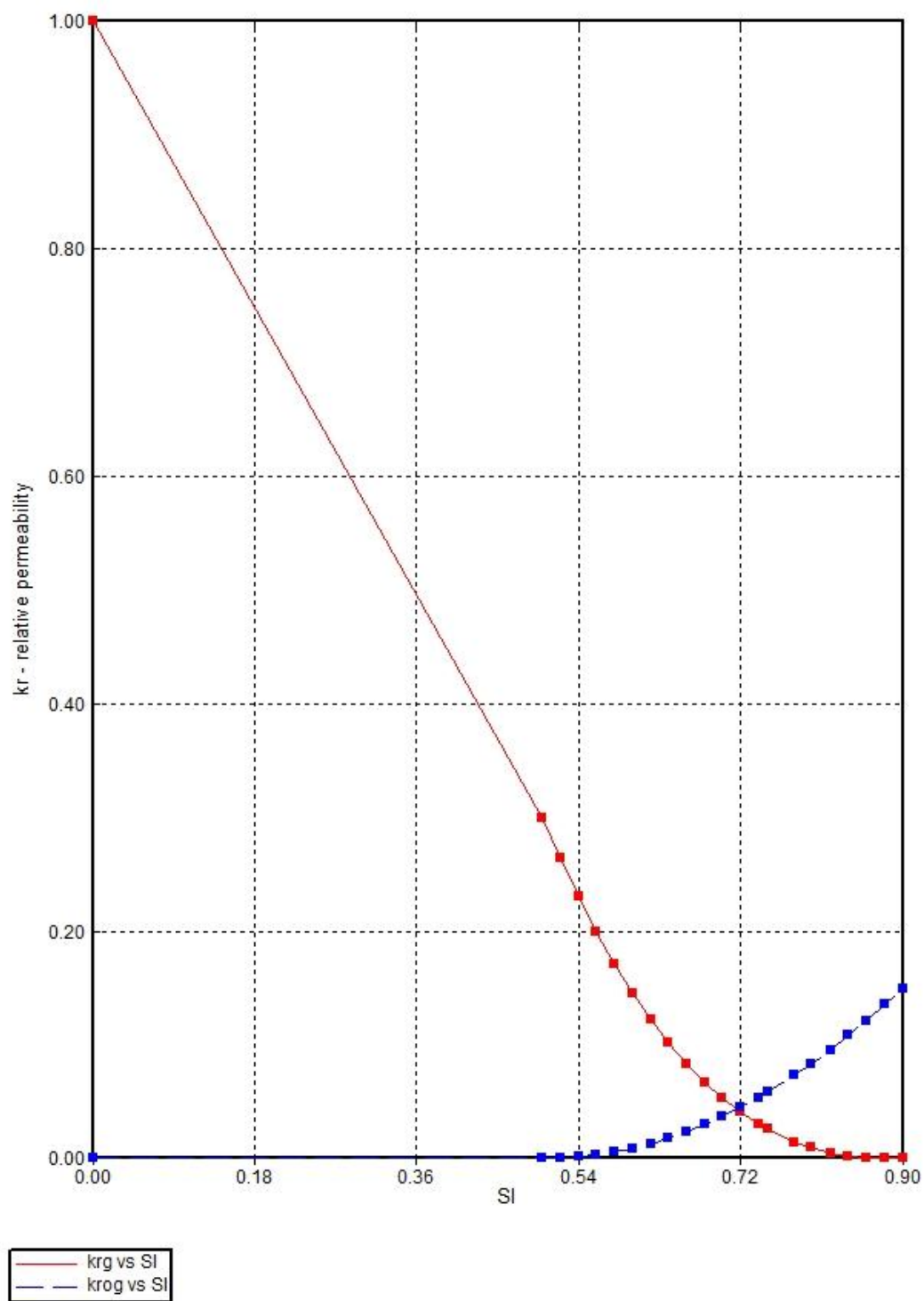


Fig. 21 – Strong liquid wetting relative permeability curve

Finally, the 10 md and 1 md field models have their production rates set to 20 million SCF/d, while the production rate of 100 md field model is increased to 100 million SCF/d to adequately model bottomhole pressure depletion.

4.2 Treatment Radius

Condensate banking will form progressively from the wellbore. This is evident from the pressure profile and liquid dropout (see **Fig. 3**). Hence, depending on the buildup of the liquid from the wellbore, it is of great interest whether or not treatment radius has any effect on the ultimate recovery. The simulation is set to compare ultimate gas recovery over a period of 20 years, with the treatment assumed to last for the entire duration.

Since the effect of the treatment is to allow smoother flow of both gas and condensates to be produced, it would logically follow then as long as treatments change a small area around the wellbore, the effect can be sustained. As seen as the results below, the assumptions hold true, at least for 1 md and 10 md reservoirs.

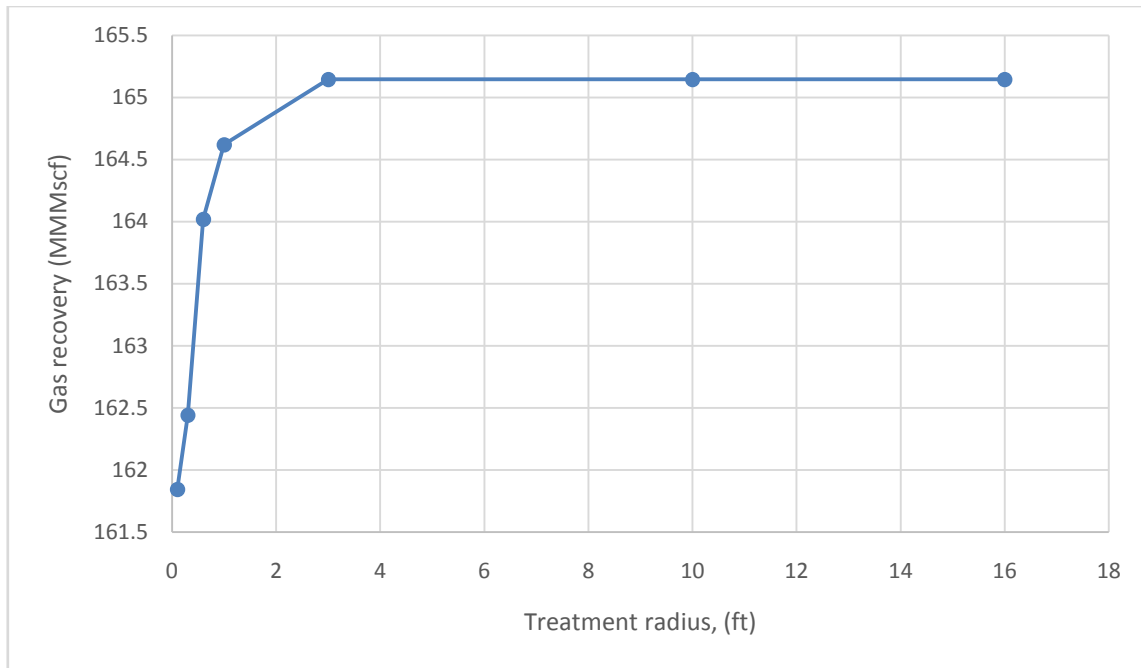


Fig. 22 – Ultimate gas recovery vs treatment radius, 10 md, intermediate gas wetting case

In **Fig. 22** above, y-axis defines the ultimate recovery in MMSCF, while the x-axis represents the treatment radius in feet. The graph denotes the ultimate recovery of the treated well for treatment radii ranging from 1 grid (0.1 feet), 2 grids (total of 0.3 feet), 3 grids (total of 0.6 feet), 4 grids (total of 1 feet), 6 grids (total of 6 feet), 15 grids (total of 10 feet), and 18 grids (16 feet). From the figure, it is clear that the gas ultimate recovery has peaked and flattened from a treatment radius of 3 feet.

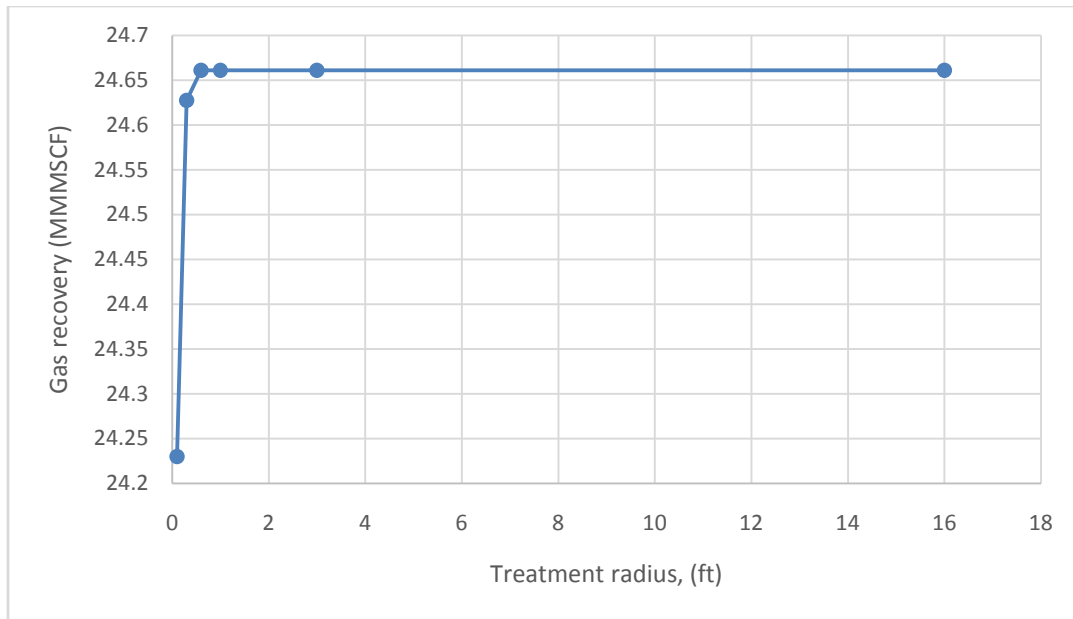


Fig. 23 – Ultimate gas recovery vs treatment radius for 1 md, intermediate gas wetting case

The trend can be seen continuing with 1 md reservoir in **Fig. 23**. It is worth noting that the ultimate recovery in this case peaks after only 3 grids (0.6ft). This is notably shorter than 10 md permeability reservoirs. 100 md reservoirs however, paint a considerably different picture as shown below.

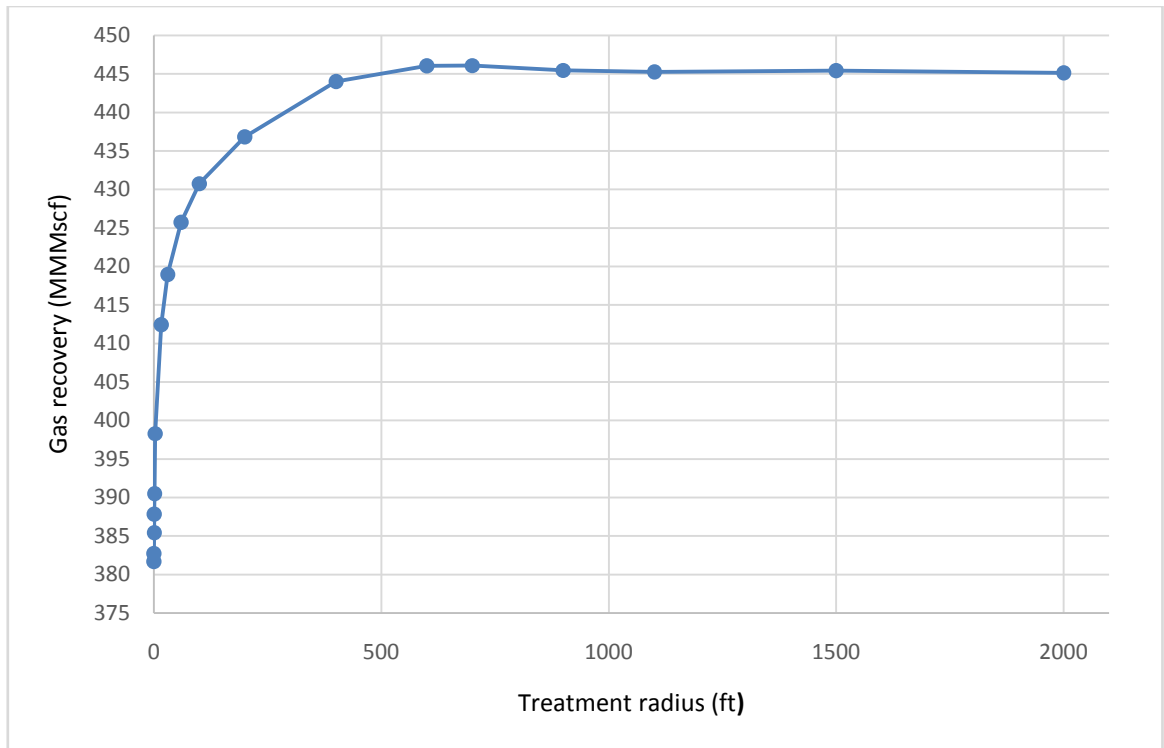


Fig. 24 – Ultimate gas recovery vs. treatment radius for 100 md, intermediate gas wetting case

Unlike simulation models with permeabilities of 1 and 10 md, the 100 md field model show a very strong correlation between increasing the treatment radius and the ultimate gas recovery. As for **Fig. 24** shows, gas produced continued to increase until 600 feet treatment radius, where it started to decline.

The results from the 100 md model may be understood in terms of production constraints. In 100 md model, the gas production rate is set to 100 MMscf/d. This

production rate causes the reservoir pressure to decrease significantly, thereby triggering more condensate buildup.

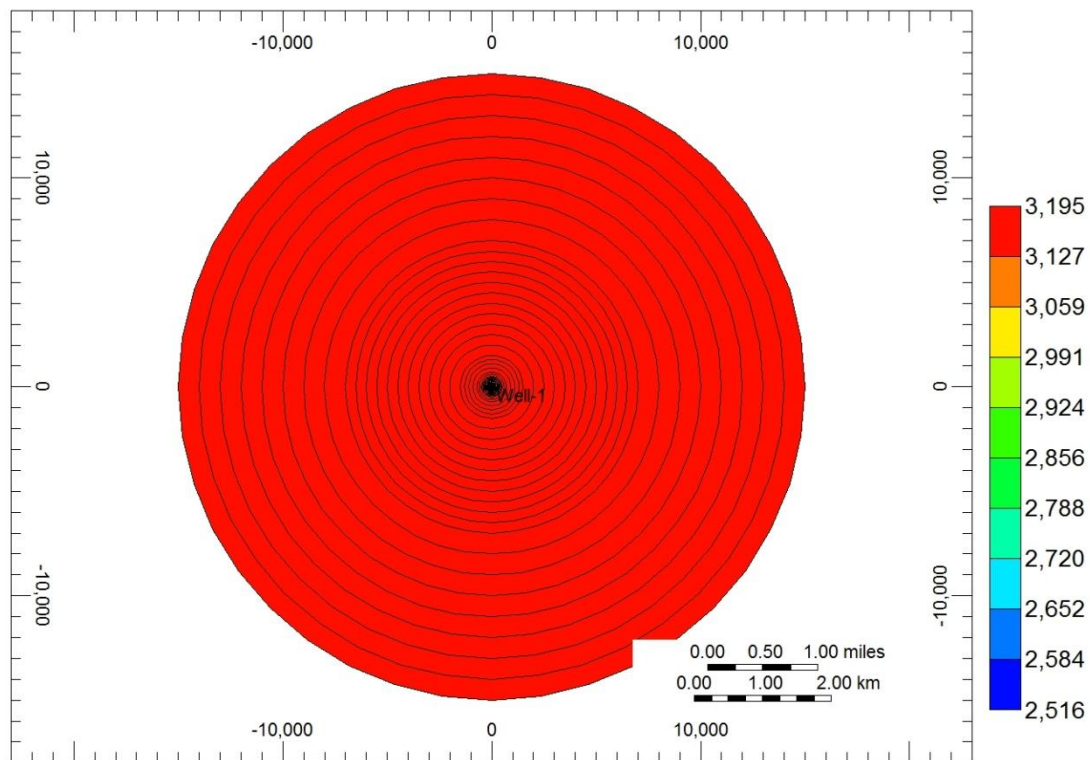


Fig. 25 – Pressure profile of 100 md model at the end of production run

Fig. 25 displays the pressure in the entirety of 100 md model at the end of a 20 year production run. The initial pressure is 5,500 psia, but after production has concluded, most of the reservoir pressure has declined to around 3,195 psia, below the dew point of 3,380 psia. At the center of the reservoir where the well is located, the pressure is even lower. The consequence of which can be seen in the figure below.

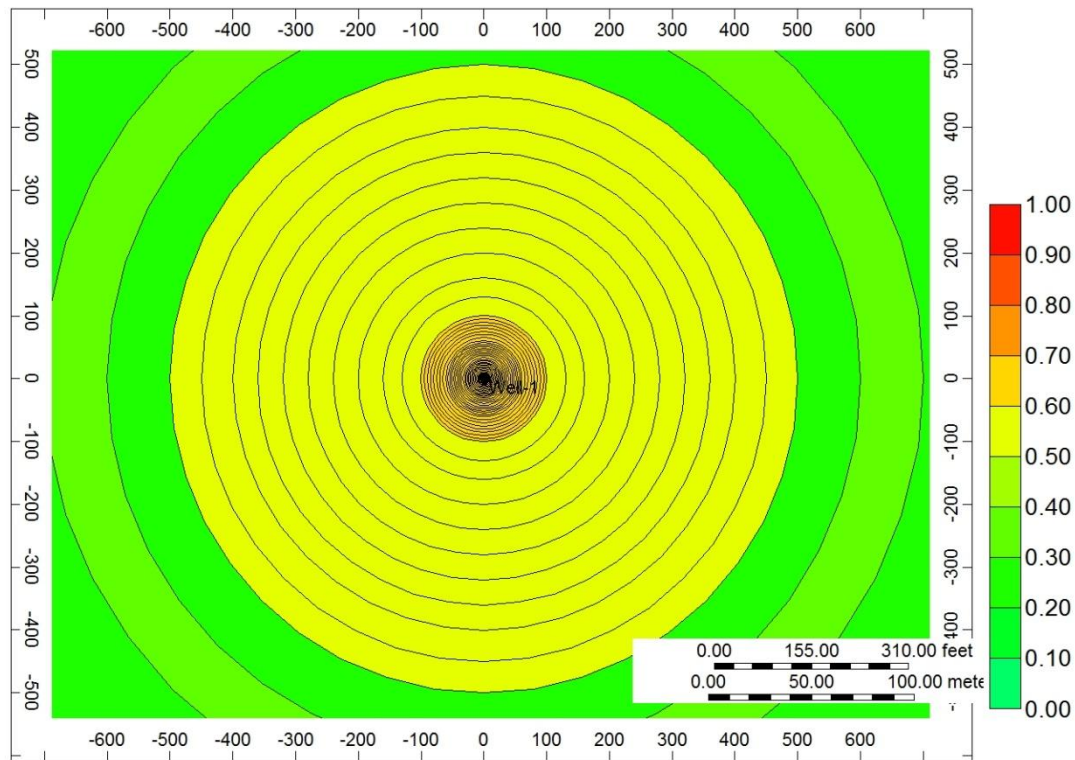


Fig. 26 – Condensate buildup radius for 100 md model at the end of production run

From **Fig. 26**, condensate build up can be clearly detected from a radius of as far as 500 feet extending from the wellbore, with higher condensate saturation at the center.

Because of the area of the condensate build up, a larger treatment radius will increase the ultimate recovery of gas at the end of the production run. In light of this, it is tempting to consider the benefits of increased production by increasing the radius of the treatment.

The next segment will deal with the implication of increasing treatment radius in terms of injection rate and downtime.

4.3 Water Injection Quantity Simulation

As a step towards an economic analysis of wettability treatment option, it is necessary to calculate the costs of such treatment. One of the appeals of near-wellbore wettability alteration is that it could be done from the producing well that is temporarily converted into an injector well, as opposed to dedicated injector wells for flooding treatments. This however, also brings the subject of a necessary halt in production, the cost of the chemical itself, as well as the injected water to carry the chemical itself.

Based on the results from the previous section, it is necessary to analyze the amount of water needed to bring the treatment to reach the optimum radius. The simulation will use the same model from Section 4.2, with several differences. First, the well model is set to an injector well. Then, the simulation runtime is decreased to 6 months, and the timesteps increased. Finally, water saturation is recorded from the edge of the treatment point.

As seen from the results of both 10 md model and 1 md model, the treatment need only reach a relatively short diameter (less than one meter). A 200 bbl/d water injection rate was chosen to investigate the time taken for the water saturation to increase to its maximum saturation at the treatment radius.

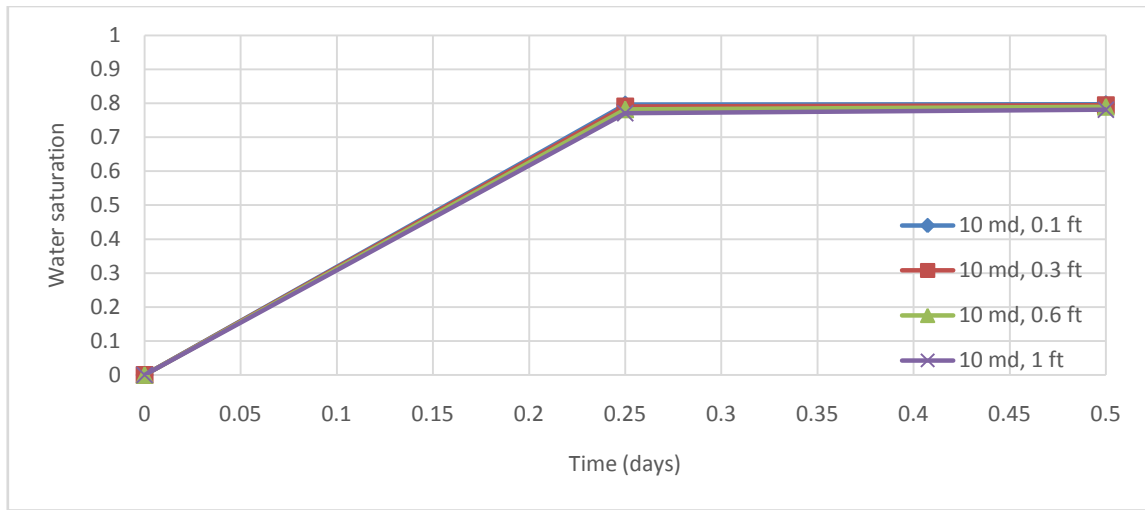


Fig. 27 – 200 bbl/d water injection on 10 md field model

As detailed on the figure above, the water saturations for the first four grids of 10 md field model were recorded. The results in **Fig. 27** show that with an injection rate of 200 bbl/d, the water saturation reaches the recommended radius within less than 6 hours.

Quite similarly, the model for 1 md in **Fig. 28** shows a very similar picture:

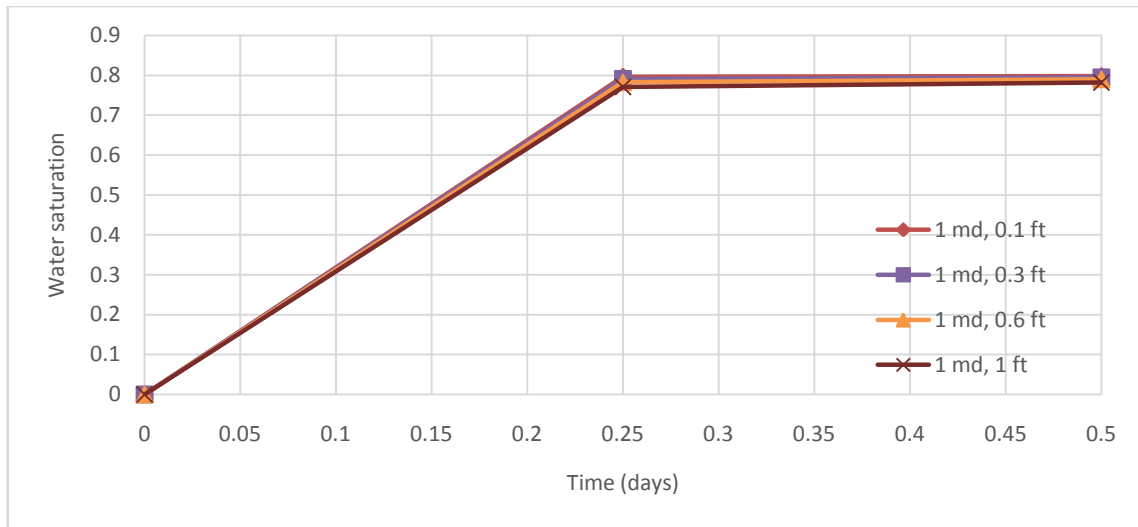


Fig. 28 – 200 bbl/d water injection on 1 md field model

While the basics of the simulation remain the same for the 100 md model, the results from Section 4.2 indicate that the farther the treatment radius goes, the better the ultimate recovery will be. However, the amount of water and time it takes can rapidly increase the costs of the treatment. Furthermore, a balance of water injection rate and treatment time taken must be achieved in order to minimize costs associated with water and chemical cost as well as production downtime resulting from treatment. Therefore, the injection analysis shall be the determining factor in deciding which radius is the most economical.

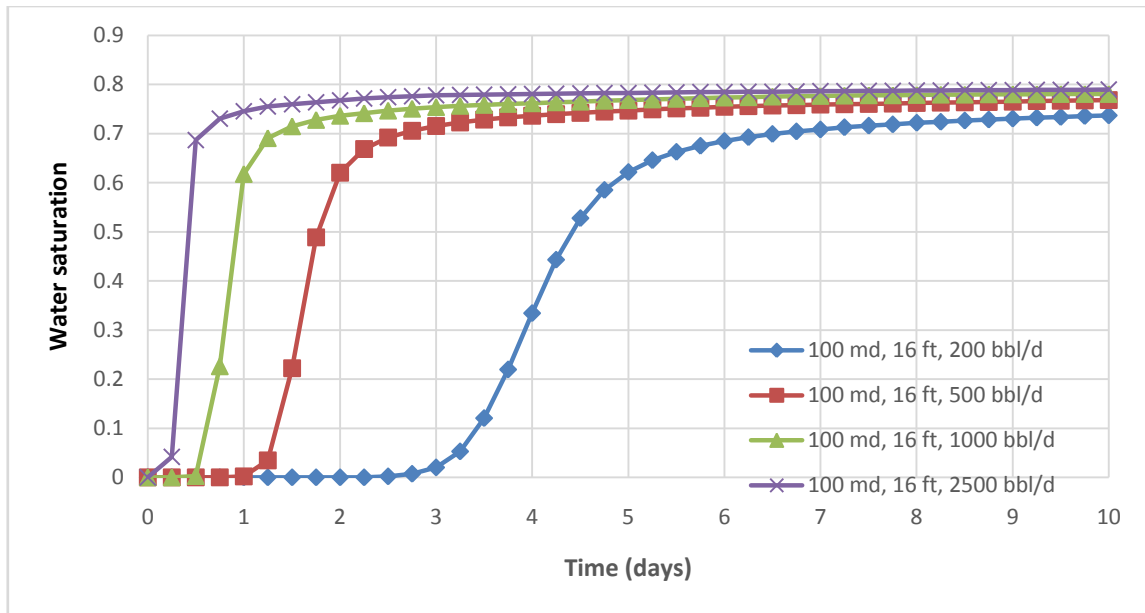


Fig. 29 – Water saturation at 16 feet vs. water injection rate for 100 md, intermediate gas case

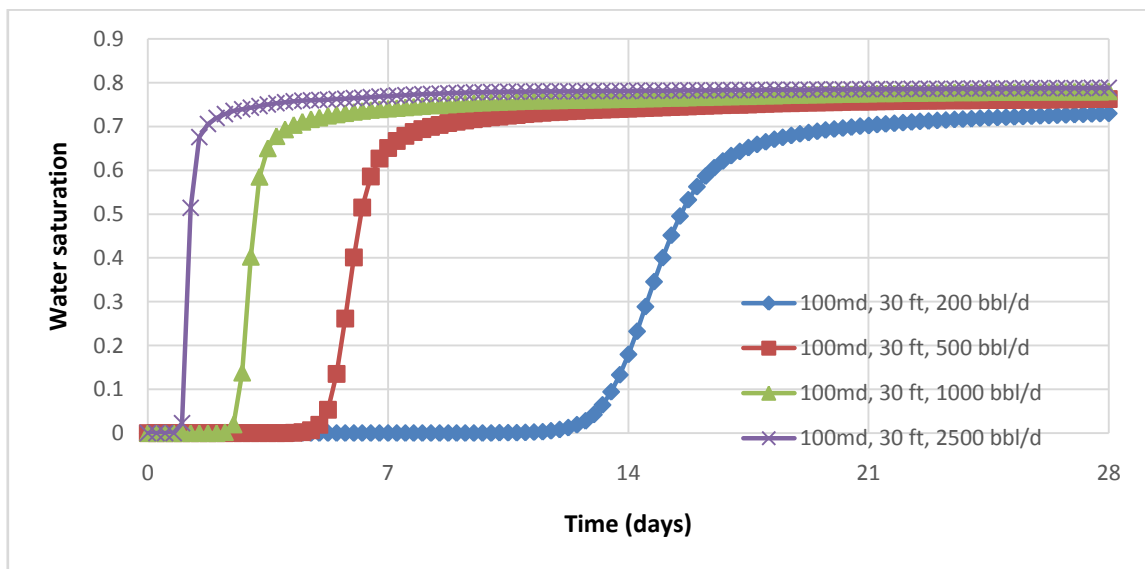


Fig. 30 – Water saturation at 30 feet vs. water injection rate for 100 md, intermediate gas case

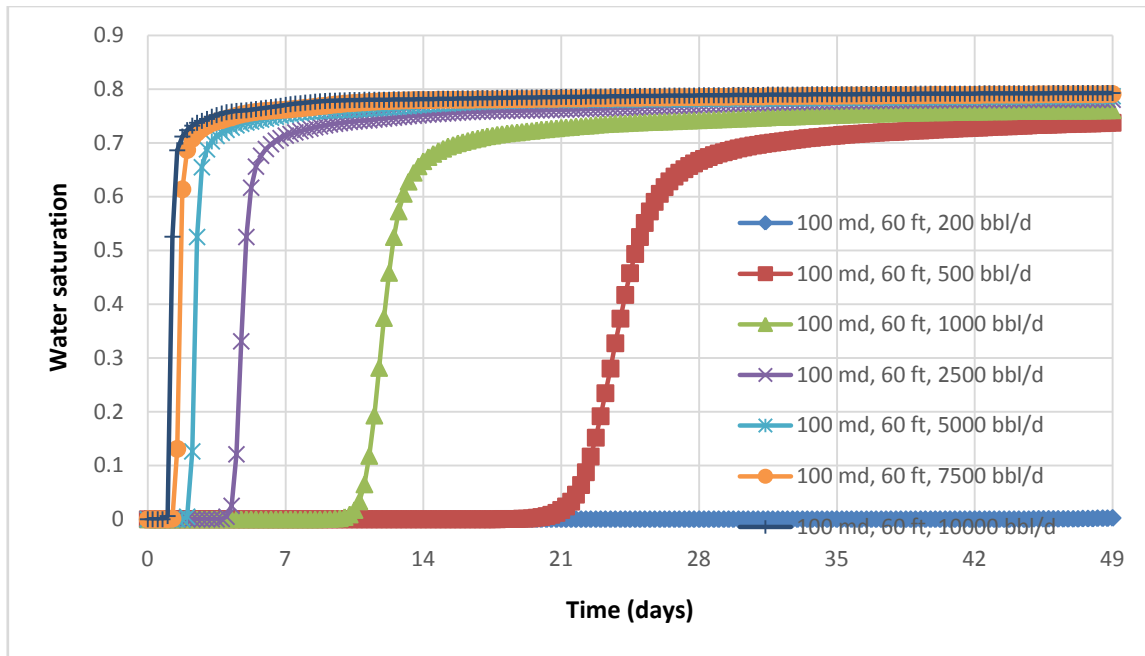


Fig. 31 – Water saturation at 60 feet vs. water injection rate for 100 md, intermediate gas case

From **figures 29 to 31**, achieving maximum water saturation within one day requires an exponentially large injection rate. For 16 feet treatment radius, 2500 bbl/d achieves maximum saturation at a reasonable 2 day period. However, at 30 feet, 2500 bbl/d injection rate maximizes the water saturation only at day 4. Furthermore, at 60 feet, an injection rate of 10,000 bbl/d is required to achieve the same saturation within 4 days. Any further increase in treatment radius will necessitate a prohibitively large volume of injected water and chemicals per day. From this, we can conclude that increasing treatment radius requires a large amount of water and surfactant to be injected to keep downtime short. The alternative is to inject at a low rate; however, this would lengthen

the downtime required for treatment and consequently increasing losses from the inability to produce during the downtime. Neither of these options is preferable; therefore, keeping treatment radius to 1 foot would be the recommended case.

4.4 Multiple-Treatment Case

One much touted aspect of wettability alteration treatment is its longevity; it is expected to last for a long time, especially in environments without water influx into the well.

That being said, it is not an unreasonable assumption that eventually, the surfactants will be desorbed from the reservoir matrix, and the near-wellbore environment will return to its default state. Hence, the possibility of multiple treatments cannot be discounted.

In this section, the simulation from Section 4.2 will be re-run, but with a scheduling pattern to simulate the need for re-treatment. The scheduling will run on intervals of one treatment every three, six, nine, and twelve months. Due to the length of the production run, it is expected that the treatment's effect on ultimate gas recovery will be significant.

The model uses the 100 md permeability to better understand the impact of reduced productivity performance against repeated treatment. Below are the results of the scheduling treatment programs for each scheduling, as well as comparison to untreated production.

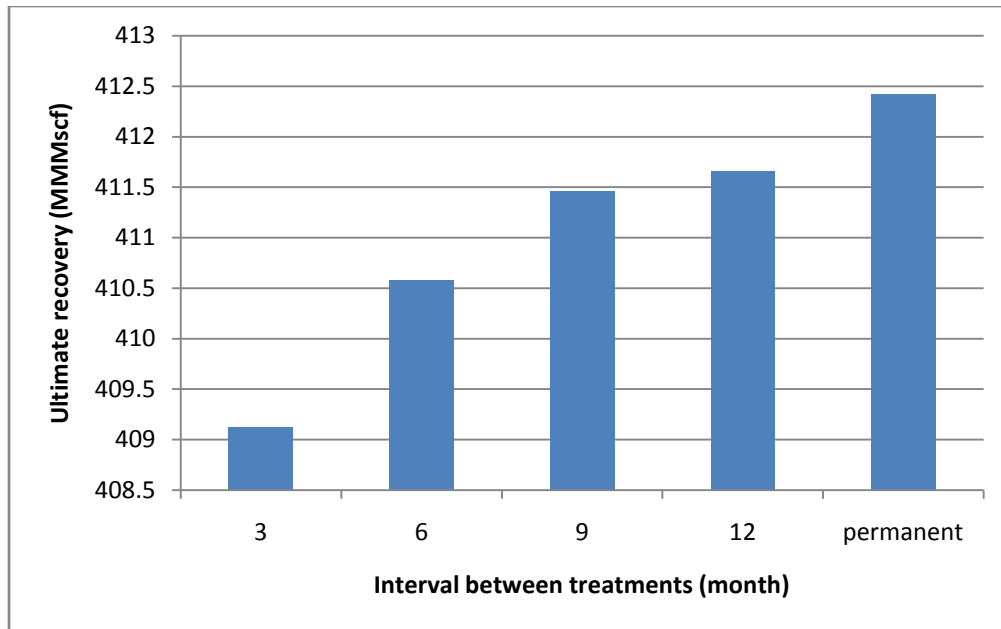


Fig. 32 – Ultimate gas recovery for varying treatment intervals, 100md intermediate wet model

It can be seen from the **Fig. 32** that the treatment frequency does have a significant effect on total production over a 20 year run. Total production is strongly negatively correlated with the number of further treatments. The production losses from each downtime accumulate and greatly affect the amount of gas recovered at the end of the production run.

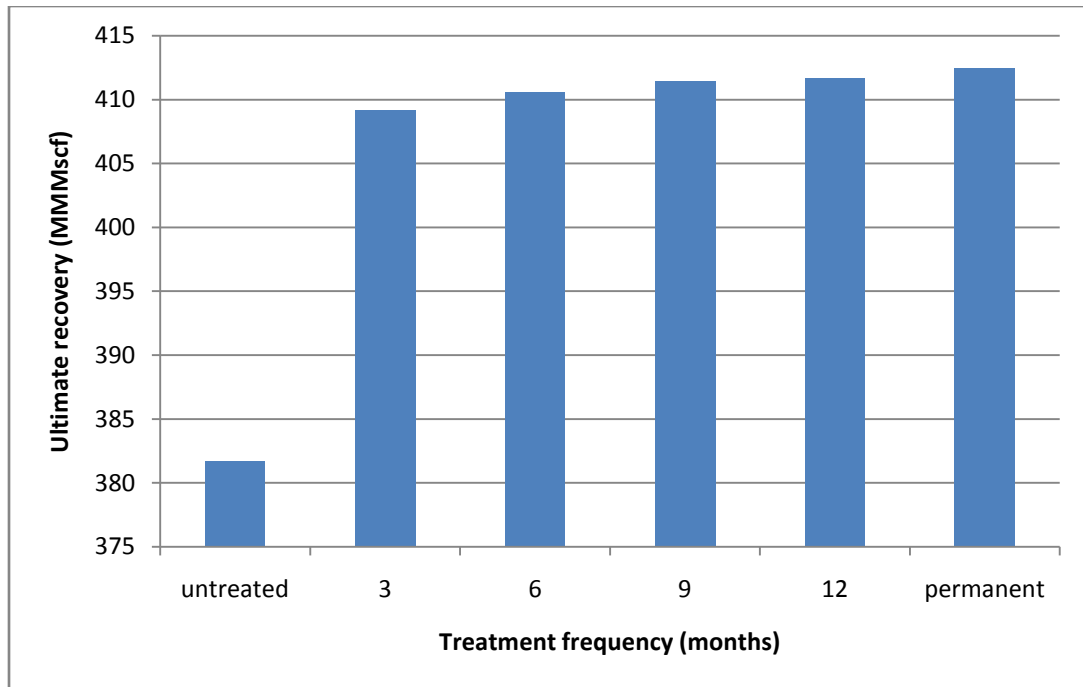


Fig. 33 – Ultimate gas recoveries of treated against untreated reservoir models for 100md, intermediate gas case

However, the result in **Fig. 33** shows that the difference in untreated and treated ultimate recoveries is significant, even when taking multiple treatments into account. This illustrates that, despite the reduction in overall gain, even repeated treatments as frequent as once every 3 months still produce better results compared to an untreated case. The next section will deal with the economic implications of this treatment option.

5. ECONOMIC ANALYSIS

5.1 Single-Treatment Case

After considering the potential gain in ultimate recovery and the associated costs for treatment, the matter immediately becomes an economic question. The worth of the treatment is not only weighed upon the ultimate increase in production, but also the costs associated with the procedure.

Gas price (USD/Mscf)		4.8
Production time (hr)		175320
Downtime for injection (hr)		72
Downtime for treatment (hr)	1 md	6
	10 md	6
	100 md, 1 feet	6
	100 md, 16 feet	48
Price of SA05611 (USD)	1 g	\$200.00
	1 bbl	\$166,880.00
	1 bbl/hr	\$6,953.33
Concentration (%)		0.7
Water Injection price (USD)	per barrel	10

Table 4 – Basic assumptions on economic analysis

From the table above, several assumptions can be drawn. Firstly, the gas price is a conservative estimate of 4.8 USD/Mscf as of May 1st, 2015 (US Energy Information Administration, 2015). Another is a higher estimate of the chemical price, which is 200 USD per one gram (Sigma-Aldrich, 2015). The treatment fluid is a highly diluted

solution, following the experimental results. Therefore, it is reasonable to assume that the density is 1 g/cc.

A crucial part in determining the profitability of the treatment is to define the expenses term. The expenses here are divided into three: Treatment Costs, Water Costs, and Downtime Cost. Treatment Cost is the primary factor of the calculation. Using a higher concentration estimate of 0.7%, it can be determined that a solution treatment injected will cost nearly \$7,000 per bbl/h. This also means that the cost will be directly proportional to the amount injected during treatment.

The second part is Water Cost. Using an estimate of \$10 per barrel, it comprises the least significant amount of expenditure associated. Lastly is Downtime Cost. Since the producing well is turned into an injector well for the purpose of the treatment, the well will not produce during that time. The “cost” here is the loss incurred by lost revenue during the time the well does not produce. Here, the calculation is obtained by multiplying the producing flow rate by the number of days the well is not producing. The downtime is assumed to take 72 hours. **Table 4** details the calculation and the costs incurred.

Permeability (md)	Injection rate (bbl/d)	Treatment Cost	Water Cost
10	200	\$8,344,000.00	\$2,000.00
1	200	\$8,344,000.00	\$2,000.00
100 ^a	200	\$8,344,000.00	\$2,000.00
100 ^b	2500	\$834,400,000.00	\$25,000.00
Permeability (md)	Lost time (d)	Production rate (scf/d)	Downtime Cost
10	3	20000000	\$288,000.00
1	3	20000000	\$288,000.00
100	3	100000000	\$1,440,000.00

Table 5 – Treatment, water, and downtime expenses. The two entries for 100 md models represent 1 foot and 16 feet treatment radii, respectively

Radius (ft)	Added Value (USD)
0.1	-\$3,411,600.00
0.3	-\$541,200.00
0.6	\$7,038,000.00
1	\$9,922,800.00
3	\$12,447,600.00

Table 6 – Profitability of treatment in 10 md cases

Radius (ft)	Added Value (USD)
0.1	-\$7,373,520.00
0.3	-\$5,466,000.00
0.6	-\$5,305,200.00

Table 7 – Profitability of treatment in 1 md cases

In **Table 6** and **Table 7**, both the 10 md and 1 md treatments resulted in a net negative income at lower radii. However, the increase in ultimate recovery could overcome the

total price imposed by the treatment; starting from 0.6 feet, the 10 md field treatments net a 7 million dollar increase in revenue.

Radius (ft)	Added Value (USD)
0.1	-\$4,760,400.00
0.3	\$8,257,200.00
0.6	\$19,830,000.00
1	\$32,588,400.00
16	-\$688,217,000.00

Table 8 – Profitability of treatment in 100md cases

In **Table 8**, the treatments for 100 md models are generally profitable, owing to the high output of the model. Of particular interest is the 16 feet treatment result. It has been established earlier in this paper that 100 md model is uniquely sensitive to increased treatment chemical reach. Despite so, calculations conclusively determined that the corresponding increase in flow rate and hence, treatment chemical, exponentially increases the expenses such that it is not profitable.

5.2 Multiple-Treatment Case

As established in the previous chapter, the possibility of multiple treatments should be considered during design stages. In particular, this serves as a worst case scenario when the initial treatment fails or otherwise does not deliver the expected results. In this section, the same methodology as the previous case will be used. The expenses terms

Treatment, Water and Downtime Costs will be utilized again. In the case of repeat treatments, all three terms will be summed up and multiplied by the number of treatments required during a 20 year production run. The total sum can be called the Unified Expenses Term. As in the simulation section, scenarios ranging from quarterly treatment to annual treatment will be explored. **Table 9** details the amount of each individual costs for each term.

Reach (ft)	Treatment Cost (USD)	Water Cost (USD)	Downtime Cost (USD)	Unified Cost Term (USD)
1	\$8,344,000.00	\$2,000.00	\$1,350,000.00	\$9,696,000.00
16	\$834,400,000.00	\$25,000.00	\$1,350,000.00	\$835,775,000.00
Interval (mo)	Duration (mo)	No. of treatments	Total Cost Term ^a (USD)	Total Cost Term ^b (USD)
3	240	80	\$775,680,000.00	\$66,862,000,000.00
6	240	40	\$387,840,000.00	\$33,431,000,000.00
9	240	26	\$252,096,000.00	\$21,730,150,000.00
12	240	20	\$193,920,000.00	\$16,715,500,000.00

Table 9 – Expenses calculation for multiple treatment cases. The Total Cost Terms

a and b refer to 1 foot and 16 feet treatment radii, respectively

Treatment interval (months)	Added Value (USD)	Added Value (USD)
3	-\$750,453,000.00	-\$66,738,425,500.00
6	-\$355,143,000.00	-\$33,300,833,000.00
9	-\$218,134,500.00	-\$21,596,041,000.00
12	-\$157,767,000.00	-\$16,580,486,500.00

Table 10 – Performance for multiple treatment case, 100 md reservoir

It can be seen clearly in **Table 10** that, with very high expense terms, a multiple treatment scenario at frequent levels is extremely unprofitable. While this is definitely connected to the high price of the treatment chemical and low selling price of gas, even an optimistic estimate of re-treatment every one year causes a considerable amount of loss.

5.3 Hypothetical Multiple-Treatment Scenario

Although looking for an economic treatment chemical is outside the scope of this thesis, it is worth looking under what conditions a repeat treatment is profitable. Many factors can increase the profitability of the treatment; gas price, lower cost chemicals, lower concentrations, lower required injected water, and others. However, from the results of previous parts, it is clear that the biggest factor in the expense term is the price of the treatment chemical, altering the chemical price has the largest effect on the treatment program.

Gas price (USD/Mscf)		4.8
Production time (hr)		175320
Downtime for injection (hr)		72
Downtime for treatment (hr)	1md	6
	10md	6
	100md, 1 feet	6
	100md, 16 feet	48
Price of surfactant (USD)	1g	\$10.00
	1 bbl	\$8,344.00
	1 bbl/hr	\$347.67
Concentration (%)		0.7
Water Injection price (USD)	per barrel	10

Table 11 – Initial conditions with reduced surfactant price

Treatment interval (mo)	Added Value (USD)	Added Value (USD)
3	-\$121,827,200.00	-\$3,322,987,200.00
6	-\$39,491,200.00	-\$1,588,555,200.00
9	-\$12,113,600.00	-\$979,760,400.00
12	\$1,379,200.00	-\$719,685,600.00

Table 12 – Profitability of hypothetical treatment using low-cost chemical

Referring to initial conditions in **Table 11**, it can be seen that, by a reduction of chemical price, an increase can be obtained in case of yearly program for one feet treatment radius (**Table 12**). On the other hand however, a quarterly treatment program is still prohibitively expensive, even with reduced chemical cost. This illustrates the importance of effective duration of the treatment, as well as the need for a low-cost chemical.

6. CONCLUSION AND RECOMMENDATIONS

Through laboratory experiments, the commercial chemical SA05611 is proven to be able to alter the wettability of a limestone rock under certain conditions. The biggest downside is the reduction of permeability due to surfactant adsorption during trials, as well as the requirement of a certain solvent formulation in order to deliver the intended result.

Using the simulation work first done by Zoghbi et al. (2010) as a basis, CMG simulations were done to analyze the effect of wettability alteration treatments in a gas condensate wells. The results indicate that the further the treatment goes, the better the ultimate recovery for a given well. This trend is most pronounced in higher permeability wells; tests using 100 md wells indicate that treatment radius of as far as 100 ft or more will have a marked increase in gas recovery. In lower permeability wells of 1 and 10 md, the effect is mostly reserved to no more than 1 to 2 feet.

The next simulation was done to analyze the impact of multiple treatments. Four different models were run through in order to determine if the ultimate recovery is affected. The results show that repeated treatments as frequent as once a month with a 3 day downtime significantly affects gas recovery at the end of the production period. However, when compared to untreated production, the ultimate recovery is demonstrably higher.

Based on the data gained from the simulations, an economic analysis was performed to determine the viability of such treatment procedures. To determine the expenditure term, the cost of chemicals, water, and downtime productivity loss is combined to form a unified cost term for calculation purposes. The results strongly indicate that for an expensive chemical, a repeat treatment option is highly uneconomical. A hypothetical scenario involving a lesser-priced surfactant shows that the treatment has potential, but the chemical must be efficient enough to last for at least a year before re-treatment if it is to be profitable.

Due to the results as well as the assumptions used in the models in these simulations, there are several recommendations for future work. Namely:

1. Finding a suitable, low-cost treatment chemical.
2. More real-life field data concerning wettability alteration on condensate gas field
3. Research onto treatment longevity, especially under adverse or unexpected conditions.
4. This simulation model assumes that once the modified wettability is set, it does not change over time. More advanced models can perhaps shed light on wettability changes post-treatment over time.

REFERENCES

- Afidick, D., Kaczorowski, N.J. and Bette, S. 1994. Production Performance of a Retrograde Gas Reservoir: A Case Study of the Arun Field. Presented at the SPE Asia Pacific Oil and Gas Conference, Melbourne, Australia, 7-10 November.
- Ahmadi, M., Sharma, M. M., Pope, G. A., Torres, D. E., McCulley, C. A., Linnemeyer, H. 2010. Chemical Treatment to Mitigate Condensate and Water Blocking in Gas Wells in Carbonate Reservoir. *SPE Prod and Oper.***26** (01): 60-667-749.SPE-133591-PA. <http://dx.doi.org/10.2118/133591-PA>
- Ahmed, T., Evans, J., Kwan, R. and Vivian, Tom. 1998. "Wellbore Liquid Blockage in Gas-Condensate Reservoirs," paper SPE 51050, presented at the SPE Eastern Regional Meeting held in Pittsburgh, PA, 9-11 November.
- Anazi, H. A., Walker, J. G., Pope, G. A., Sharma, M. M., Hackney, D. F. 2005. A Successful Methanol Treatment in a Gas/Condensate Reservoir: Field Application. *SPE Prod and Fac.* **20** (01): 60-69.SPE-80901-PA-P. <http://dx.doi.org/10.2118/80901-PA>
- Bang, V., Pope, G. A., Sharma, M. M., et al. 2010. A New Solution to Restore Productivity of Gas Wells with Condensate and Water Blocks. *SPE Res Eval and Eng.***13** (02): 323-331.SPE-116711-PA. <http://dx.doi.org/10.2118/116711-PA>
- Barnum, R.S., Brinkman, F.P., Richardson, T.W. and Spillette, A.G. 1995. Gas Condensate Reservoir Behaviour: Productivity and Recovery Reduction Due to Condensation. Presented at the SPE Annual Technical Conference and Exhibition, Dallas, Texas, 22-25 October.

- Benesch, J., Gahr, J.Z., Schmidt, M.H. and Al-Mohsin, A.H. 2007. Optimization Of High Pressure, High Rate (HPHR) Gas Wells In A Giant Offshore Field. Presented at the SPE Middle East Oil and Gas Show and Conference, Manama, Bahrain, 11-14 March.
- Butler, M. L., Trueblood, J. L., Pope, G. A., Sharma, M. M., Baran Jr., J. R., Johnson, D. 2009. A Field Demonstration of a New Chemical Stimulation Treatment for Fluid-Blocked Wells. Paper presented at the 2009 SPE Annual Technical Conference and Exhibition, New Orleans, Louisiana, USA, 4-7 October 2009.SPE-120577-MS. <http://dx.doi.org/10.2118/120577-MS>
- Chukwudeme, E. A., Fjelde, I., Abeysinghe, K., Lohne, A. 2013. Effect of Interfacial Tension on Water/Oil Relative Permeability on the Basis of History Matching to Coreflood Data.*SPE Res Eval and Eng.***17** (01): 37-48. SPE-143028-PA. <http://dx.doi.org/10.2118/143028-PA>
- Engineer, R. 1985. Cal Canal Field, California: Case History of a Tight and Abnormally Pressured Gas Condensate Reservoir. Presented at the SPE California Regional Meeting, Bakersfield, California, 27-29 March.
- Evans, D.F. and Wennerström, H. 1994. In *The Colloidal Domain, Where Physics, Chemistry, Biology, and Technology Meet.*, pp. 456-457. New York.: John Wiley and Sons, Inc
- Fahes, M., Firoozabadi, A. 2007. Wettability Alteration to Intermediate Gas-Wetting in Gas-Condensate Reservoirs at High Temperatures. *SPE J***12** (04): 397-407.SPE-96184-PA. <http://dx.doi.org/10.2118/96184-PA>

- Fan, L., Harris, B.W., Jamaluddin, A. et al. 2005. Understanding Gas-Condensate Reservoirs. *Oilfield Review* **Winter**: 14-27.
- Fernandez, R., Fahes, M., Zoghbi, B., El Cheikh Ali, N. 2011. Wettability Alteration at Optimum Fluorinated Polymer Concentration for Improvement in Gas Mobility. Paper presented in SPE EUROPE/EAGE Annual Conference and Exhibition, Vienna, Austria, 23-26 May 2011.SPE-143040-MS.
<http://dx.doi.org/10.2118/143040-MS>
- Hirasaki, G.J., Pope, G. A., 1974. Analysis of Factors Influencing Mobility and Adsorption in the Flow of Polymer Solution Through Porous Media.*SPE J***14** (04): 337-346 SPE-4026-PA. <http://dx.doi.org/10.2118/4026-PA>
- Holmberg, K., Jönsson, B., Kronberg, B. and Lindman, B. 2002. Surfactants and Polymers in Aqueous Solution. West Sussex, England: John Wiley & Sons, Ltd.
- Jamaluddin, A.K.M., Thomas, S.Y.J., D’Cruz, D., and Nighswander, J. 2001. “Experimental and Theoretical Assessment of Using Propane to Remediate Liquid Buildup on Condensate Reservoirs.” Paper SPE 71526 presented at the SPE Annual Technical Conference and Exhibition, New Orleans, LO, September 30 – October 3.
- Kumar, V., Pope, G.A. and Sharma, M.M. 2006. "Improving the Gas and Condensate Relative Permeability Using Chemical Treatments", SPE 100529 presented at the 2006 SPE Gas Technology Symposium, Calgary, Alberta, Canada, May 15-17.

- Kumar, K., Dao, E. K., Mohanty, K. K. 2008. Atomic Force Microscopy Study of Wettability Alteration by Surfactants. *SPE J13* (02): 137-145. SPE-93009-PA. <http://dx.doi.org/10.2118/93009-PA>
- Mahadevan, J., Sharma, M. M. 2005. Factors Affecting Clean-up of Water-Blocks: A Laboratory Investigation. *SPE J10* (03): 238-246. SPE-84216-PA. <http://dx.doi.org/10.2118/84216-PA>
- McCain, W. 1990. *The Properties of Petroleum Fluids*. Tulsa, Oklahoma: PennWell Publishing Company.
- Mohan J., G.A. Pope, and M.M. Sharma. 2006. “Effect of Non-Darcy Flow on Well Productivity in a Hydraulically Fractured Gas/Condensate Well”, SPE Paper 103025, SPE Annual Technical Conference and Exhibition, San Antonio, TX, 24-27 September.
- Noh, M., Firoozabadi, A. 2008. Wettability Alteration in Gas-Condensate Reservoirs to Mitigate Well Deliverability Loss by Water Blocking. *SPE Res Eval and Eng.* **2** (04): 676-685. SPE-98375-PA <http://dx.doi.org/10.2118/98375-PA>
- Rao, D. N., Ayirala, S. C., Abe, A. A., et al. 2006. Impact of Low-Cost Dilute Surfactants on Wettability and Relative Permeability. Paper prepared for 2006 SPE/DOE Symposium on Improved Oil Recovery at 22-26 April, Tulsa, Oklahoma, USA. SPE-99609-MS. <http://dx.doi.org/10.2118/99609-MS>
- Sharma, G., Mohanty, K. K. 2013. Wettability Alteration in High-Temperature and High-Salinity Carbonate Reservoirs. *SPE J18* (04): 646-655. SPE-147306-PA. <http://dx.doi.org/10.2118/147306-PA>

Sigma-Aldrich Corporation. 2015. 05611 Fluka.

<http://www.sigmaaldrich.com/catalog/product/fluka/05611>. Accessed 1 May 2015.

Smits, R.M.M., van der Post, N. and al Shaidi, S.M. 2001. Accurate Prediction of Well Requirements in Gas Condensate Fields. Presented at the SPE Middle East Oil Show, Manama, Bahrain, 17-20 March. 10.2118/68173-MS.

Tang, G.Q., Firoozabadi, A. 2002. Relative Permeability Modification in Gas/Liquid Systems Through Wettability Alteration to Intermediate Gas Wetting. *SPE Res Eval and Eng.* **5** (06): 427-436. SPE-81195-PA <http://dx.doi.org/10.2118/81195-PA>

Thomas, F.B., Anraku, T., Bennion, D.B. and Bennion, D.W. 1996. Optimizing Production From A Rich Gas Condensate Reservoir. Presented at the SPE/DOE Improved Oil Recovery Symposium, Tulsa, Oklahoma, 21-24 April.

Trogus, F. J., Sophany, T., Schechter, R. S., et al. 1977. Static and Dynamic Adsorption of Anionic and Nonionic Surfactants. *SPE J* **17** (05): 337-344. SPE-6004-PA. <http://dx.doi.org/10.2118/6004-PA>

United States Natural Gas Industrial Price (Dollars per Thousand Cubic Feet). US Energy Information Administration. 30 April 2015. <http://www.eia.gov/dnav/ng/hist/n3035us3m.htm>. Accessed 1 May 2015.

Wheaton, R.J. and Zhang, H.R. 2000. Condensate Banking Dynamics in Gas Condensate Fields: Compositional Changes and Condensate Accumulation Around

Production Wells. Presented at the SPE Annual Technical Conference and Exhibition, Dallas, Texas, 1-4 October.

Wu, S. Firoozabadi, A. 2011. Simultaneous Increase in Gas and Liquid Relative Permeabilities and Reduction of High-Velocity Coefficient from Wettability Alteration. *J Can Pet Technol.***50** (02): 17-23.SPE-144637-PA.
<http://dx.doi.org/10.2118/144637-PA>

Xu, W., Ayirala, S. C., Rao, D. N. 2008. Measurement of Surfactant-Induced Interfacial Interactions at Reservoir Conditions. *SPE Res Eval and Eng.***11** (01): 83-94.SPE-96021-PA. <http://dx.doi.org/10.2118/96021-PA>

Zoghbi, B., Fahes, M.M. and Nasrabadi, H. 2010. Identifying the Optimum Wettability Conditions for the Near-Wellbore Region in Gas-Condensate Reservoirs. Presented at the Tight Gas Completions Conference, San Antonio, Texas, USA, 2-3 November.

APPENDIX A

ADDITIONAL EXPERIMENTAL RESULTS OF CORE TREATMENTS USING SA05611

Below are the decane imbibition results of experiments 8-12 using cores treated with SA05611. All of them are treated under room temperature and pressure conditions.

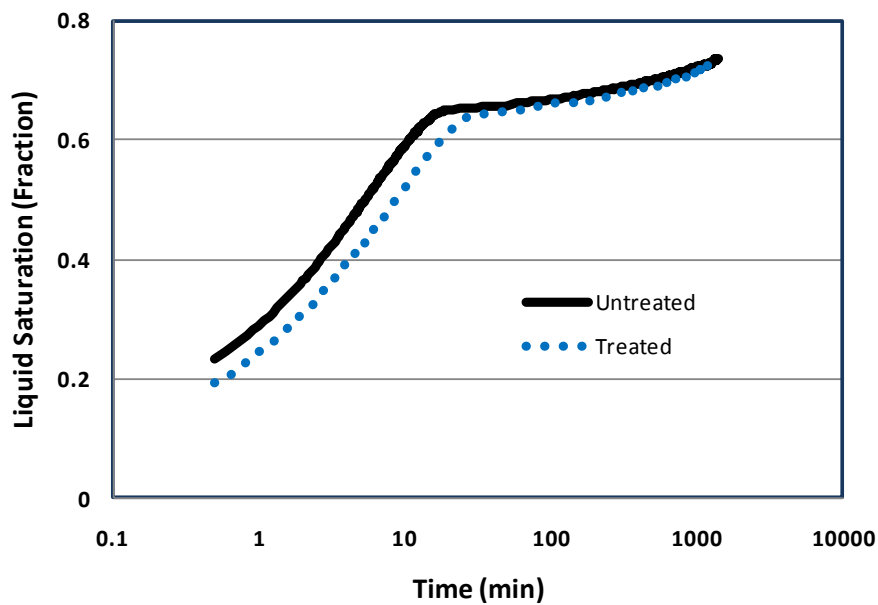


Fig. A-1 – Decane saturation vs. time for rock ILY35 treated at 24°C with 0.49% SA05611, 0.74% NaHCO₃, 49.4% Methanol, and 49.4% Water.

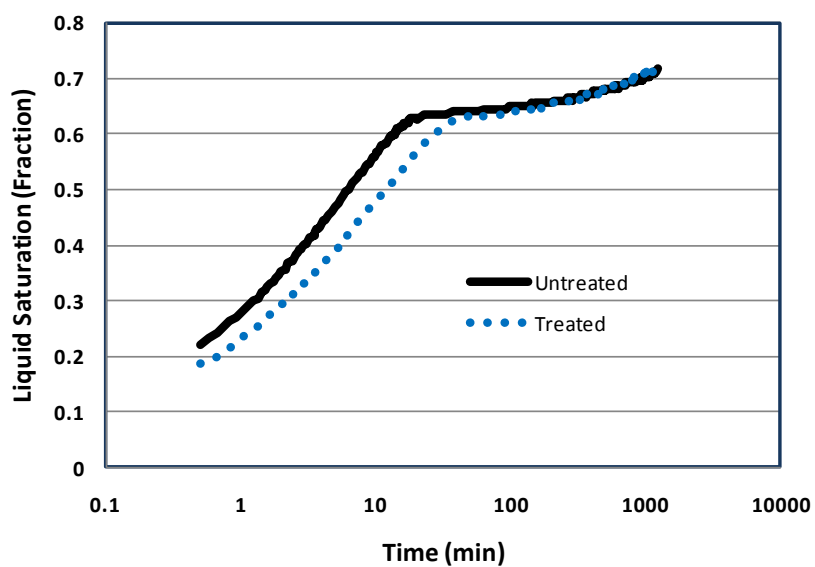


Fig. A-2 – Decane saturation vs. time for rock ILY29 treated at 24°C but aged at 100°C with 0.5% SA05611, 0.5% NaHCO₃, 49.5% Methanol, and 49.5% Water

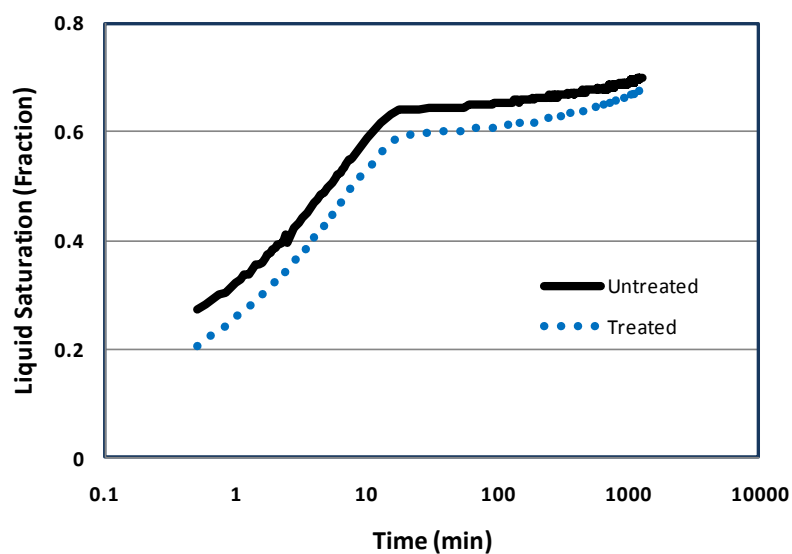


Fig. A-3 – Decane saturation vs. time for rock ILY36 treated at 24°C with 0.49% SA05611, 0.74% NaHCO₃, 49.4% Isopropyl Alcohol, and 49.4% Water

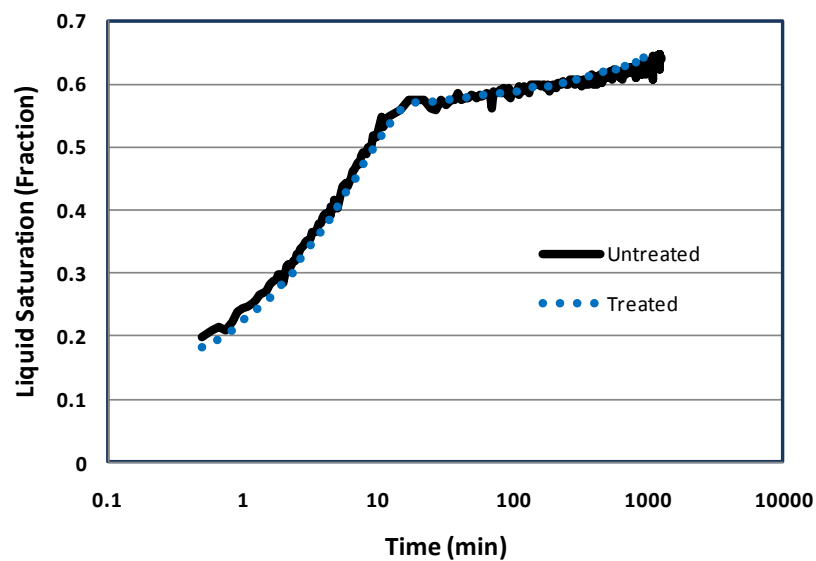


Fig. A-4 – Decane saturation vs. time for rock ILY24A treated at 24°C with 0.98% SA05611, 0.98% NaHCO₃, 49% Isopropyl Alcohol and 49% Water

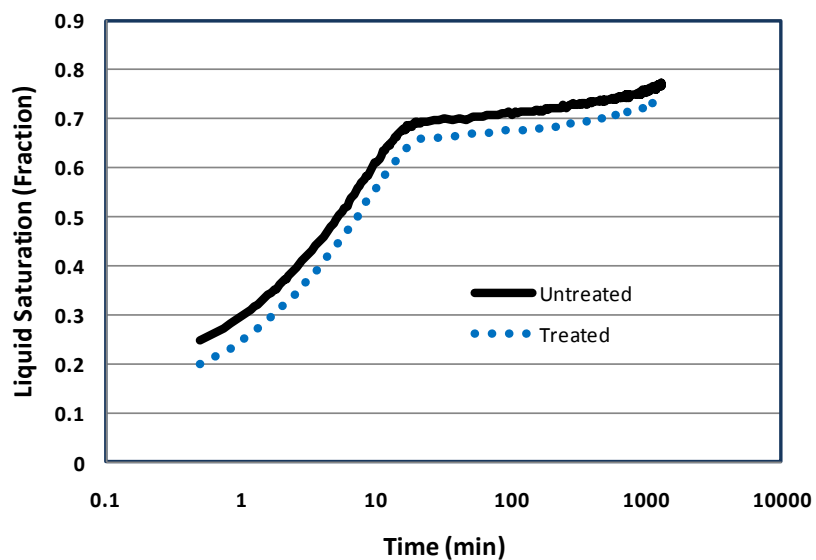


Fig. A-5 – Decane saturation vs. time for rock ILY27 treated at 24°C with 0.47% SA05611, 0.47% NaHCO₃, 47% Isopropyl Alcohol, 47% Water and 5% Ethanol

APPENDIX B

GLASS PLATE CONTACT ANGLE EXPERIMENTS

In order to have a better understanding of the effect of the various components in the treatment mixture, a different type of experiment was done by treating glass plates shown in **Fig. B-1**. The goal was to have a quick test where several mixtures can be tested at the same time using a minimal amount of chemical. Glass plates measuring around 1" x 3" was immersed in a solution and aged overnight before drying and testing. In order to minimize the amount of solution needed, a small pocket was prepared using paper and tape and the glass plate was aged in it overnight inside a plastic cup to avoid evaporation (**Figs. B-1a** and **B-2b**).

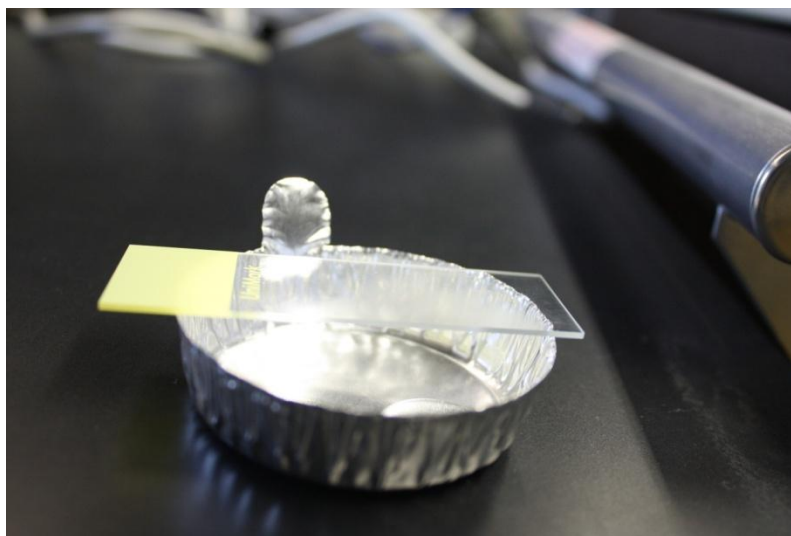


Fig. B-1 – Glass plates used in glass treatment experiment

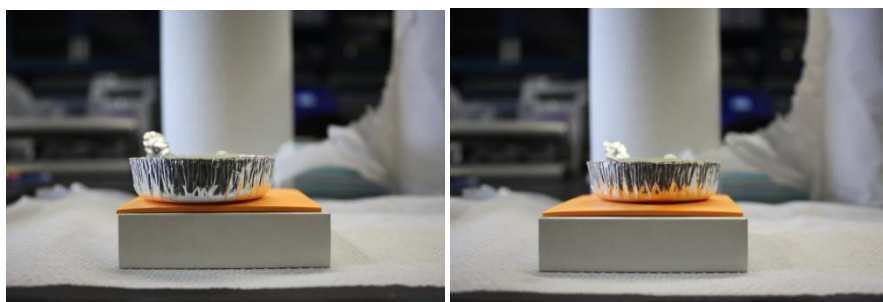


Fig. B-2 – A photo of the glass plates (a) that were treated with various mixtures and the aging process (b) in a paper pocket inside a closed plastic cup

The list of mixtures that were used in this experiment is presented in **Table B-1**. The table also shows the result of contact angle measurements after the aging period of around 15 hours was completed and the glass plates were dried in the oven for two hours at 140°C. A couple of examples of the contact angle measurements are shown in **Fig. B-3**. Plate #1 was used as a reference. Plates #2 and #3 were aged in Methanol and Water respectively without any additives. Plates #4 and #5 were aged in Methanol with 0.5% SA05611 and Water with 5% NaHCO_3 respectively. Plates #6, #7 and #8 were aged in mixtures including both the surfactant and the salt.

<u>Number</u>	<u>Mixture</u>	<u>Water Angle</u>	<u>Decane Angle</u>
1	None	15°	30°
2	Methanol	20°	3°
3	Water	20°	3°
4	2 cc Methanol and 0.01g SA05611	30°	30°
5	4 cc Water and 0.2g NaHCO ₃	10°	25°
6	1 cc Methanol, 0.01g SA05611 +2 cc Water, 0.01g NaHCO ₃	15°	50°
7	1 cc Methanol, 0.01g SA05611 +3 cc Water, 0.1g NaHCO ₃	0°	70°
8	0.5 cc Methanol, 0.01g SA05611 +3 cc Water, 0.1g NaHCO ₃ , 0.5 cc Ethanol	5°	45°

Table B-1 – GLASS PLATE EXPERIMENTS



(a) glass plate #6

(b) glass plate #7

Fig. B-3 – Photos for a drop of decane on glass plates after aging in various solutions. (a) an angle of 50° is observed and (b) an angle of 70° is observed

The following conclusions were drawn from the results presented in **Table 9** of the contact angle measurements:

- Aging plate #1 at high temperature increased the contact angle in decane from $\sim 3^\circ$ to 30° although the plate was not aged in any solution.
- Exposing plates #2 and #3 to methanol and water preserved the low angle of $\sim 3^\circ$ even after aging at high temperature.
- The use of higher concentrations of NaHCO_3 (plates #5, #7 and #8) resulted in a lower angle in water, indicating a change towards increased water-wetting.
- The use of a higher concentration of salt, plate #7, resulted in a better treatment than that of plate #6.
- The addition of ethanol to the mixture (plate #8) reduced the effectiveness of the treatment.

APPENDIX C

UNIFIED COST TERM EQUATION

The following equation is formulated as a simple, non-simulation projected gain if multiple treatments using wettability-altering surfactants are required for a gas condensate well.

$$P = \Delta - \frac{t_p}{\alpha} \times \beta - \gamma \quad (C.1)$$

The terms are explained below:

Δ = gross treatment payout (USD) = $(\Sigma p_n - \Sigma p_0) \times Y_{\text{gas}}$

α = treatment frequency (months)

β = standardized expense term (USD)

$\beta = (t_{\text{np}} \times Q_{\text{gas}} \times Y_{\text{gas}}) + \left(\frac{Q_{\text{water}}}{5.615} \times c_{\text{surf}} \times Y_{\text{surf}} \right) + (Y_{\text{water}} \times Q_{\text{water}})$

γ = fractional OPEX (USD) = $0.8 \times Y_{\text{gas}}$

t_p = production time (months)

t_{np} = nonproducing time (months) = sum of shut-in, switching, and treatment time

Σp_n = projected cumulative production using treatment regiment n (MMMscf)

Σp_0 = projected cumulative production with base production case (MMMscf)

Y_{gas} = gas price (USD)

Y_{surf} = surfactant price (USD)

Y_{water} = water price (USD)

c_{surf} = volume fraction concentration of surfactant

Q_{gas} = production rate of gas ($\frac{\text{scf}}{\text{d}}$)

Q_{water} = injection rate of water ($\frac{\text{bbl}}{\text{d}}$)

Assumptions:

- gas price is constant throughout the years
- term γ (fractional OPEX) is an assumed quantity
- nonproducing time is not subtracted from production time
- gas production rate used in calculation of unified expense term is taken from base case simulation if no downtime occurs
- treatment frequency time is an integer, and thus, must be rounded down
- does not take interest and change of price/expenses over the years into account

APPENDIX D

GRID SIZE TABLE

<i>Grids</i>	<i>Increment (ft)</i>	<i>Total radius</i>	<i>Grids</i>	<i>Increment (ft)</i>	<i>Total radius</i>
1	0.1	1.3	14	1	158
2	0.2	4	15	1	199
3	0.3	8.2	16	2	244
4	0.4	14	17	2	292
5	0.5	21.5	18	2	343
6	0.5	30.5	19	2	397
7	0.5	41	20	2	454
8	0.5	53	21	2	514
9	1	68	22	2	577
10	1	85	23	2	643
11	1	104	24	2	714
12	1	125	25	2	788
13	1	148	26	3	867
<i>Grids</i>	<i>Increment (ft)</i>	<i>Total radius</i>	<i>Grids</i>	<i>Increment (ft)</i>	<i>Total radius</i>
27	3	950	40	5	6022
28	3	992	41	5	6682
29	3	1140	42	5	6782
30	3	1342	43	5	6887
31	3	1548	44	30	7047
32	3	1858	45	30	7237
33	3	2172	46	40	7477
34	3	2490	47	40	7757
35	3	2812	48	40	8077
36	5	3442	49	40	8437
37	5	4078	50	40	8837
38	5	4720	51	40	9277
39	5	5368	52	50	9777
<i>Grids</i>	<i>Increment (ft)</i>	<i>Total radius</i>	<i>Grids</i>	<i>Increment (ft)</i>	<i>Total radius</i>
53	50	10327	66	500	45427
54	100	11027	67	500	51427

55	100	11827	68	500	57927
56	200	12927	69	500	64927
57	200	14227	70	500	72427
58	200	15727	71	1000	81427
59	200	17427	72	1000	91427
60	500	19927	73	1000	102427
61	500	22927	74	1000	114427
62	500	26427	75	1000	127427
63	500	30427	76	1000	141427
64	500	34927	77	1000	156427
65	500	39927	78	1000	172427

Table D-1. Grid size distribution and total length

APPENDIX E

SAMPLE SIMULATION CODE

The following is a sample code used for the simulation. This particular code is used in Section 5.3 for permanent treatment case.

```
DIM MDDD 3159
DIM MDV 351
INUNIT FIELD
WSRF WELL 1
WSRF GRID TIME
OUTSRF GRID PRES SG SO SW
OUTSRF RES NONE
WPRN GRID 0
OUTPRN GRID NONE
OUTPRN RES NONE
**$ Distance units: ft
RESULTS XOFFSET      0.0000
RESULTS YOFFSET      0.0000
RESULTS ROTATION      0.0000 **$ (DEGREES)
RESULTS AXES-DIRECTIONS 1.0 -1.0 1.0
```

**\$

**\$ Definition of fundamental cylindrical grid

**\$

GRID RADIAL 78 1 1 *RW 0.33

KDIR DOWN

DI IVAR	0.1	0.2	0.3	0.4
0.5	0.5	0.5	0.5	1
1	1	1	1	1
1	2	2	2	2
2	2	2	2	2
2	3	3	3	3
3	3	3	3	3
3	5	5	5	5
5	5	5	5	30
30	40	40	40	40
40	40	50	50	100
100	200	200	200	200
500	500	500	500	500

500	500	500	500	500
500	1000	1000	1000	1000
1000	1000	1000	1000	

DJ JVAR 360

DK ALL

78*70

DTOP

78*8000

**\$ Property: NULL Blocks Max: 1 Min: 1

**\$ 0 = null block, 1 = active block

NULL CON 1

**\$ Property: Porosity Max: 0.12 Min: 0.12

POR CON 0.12

**\$ Property: Permeability I (md) Max: 100 Min: 100

PERMI CON 100

PERMJ EQUALSI

PERMK EQUALSI

**\$ Property: Pinchout Array Max: 1 Min: 1

**\$ 0 = pinched block, 1 = active block

PINCHOUTARRAY CON 1

CPOR 1e-6

**The following is the fluid component

**property data in GEM format.

**The unit system and fluid compositions should

**be specified in the I/O control section.

**The units and compositions specified in WinProp

**are included here as comments for informational purposes.

** PVT UNITS CONSISTENT WITH *INUNIT *FIELD

**COMPOSITION *PRIMARY

** 6.7930000E-01 9.9000000E-02 5.9100000E-02 7.8600000E-02

** 1.8100000E-02 5.1800000E-02 1.4100000E-02

**COMPOSITION *SECOND

** 9.4680000E-01 5.2700000E-02 5.0000000E-04 0.0000000E+00

** 0.0000000E+00 0.0000000E+00 0.0000000E+00

**\$ Model and number of components

MODEL PR

NC 7 7

COMPNAME 'C1+N2' 'C2+CO2' 'C3' 'C4+C5' 'C6' 'C7-C12' 'C13+'

HCFLAG

0 0 0 0 0 0

VISCOR HZYT

MIXVC 1

VISCOEFF 1.0230000E-01 2.3364000E-02 5.8533000E-02 -4.0758000E-02

9.3324000E-03

MW

1.6385000E+01 3.1774000E+01 4.4097000E+01 6.2925000E+01 8.6000000E+01

1.1902000E+02 2.1712000E+02

AC

0.0089 0.1135 0.152 0.2029 0.2637 0.3346 0.5972

PCRIT

4.5080000E+01 5.0360000E+01 4.1900000E+01 3.5610000E+01 3.2460000E+01

2.6960000E+01 1.9300000E+01

VCRIT

9.9000000E-02 1.4100000E-01 2.0300000E-01 2.7400000E-01 3.4400000E-01

4.7000000E-01 7.4900000E-01

TCRIT

1.8870000E+02 3.0530000E+02 3.6980000E+02 4.3390000E+02 5.0750000E+02

5.8670000E+02 7.2930000E+02

PCHOR

40.9 89 150.3 183.1 250.1 341.9 586.2

SG

0.26214 0.44809 0.507 0.59121 0.68013 0.75386 0.8667

TB

-259.039 -132.181 -43.7 42.739 142.201 263.454 501.416

OMEGA

0.457236 0.457236 0.457236 0.457236 0.457236 0.457236 0.457236

OMEGB

0.0777961 0.0777961 0.0777961 0.0777961 0.0777961 0.0777961 0.0777961

VSHIFT

0 0 0 0 0 0

VISVC

9.9000000E-02 1.4100000E-01 2.0300000E-01 2.7400000E-01 3.4400000E-01

4.7000000E-01 7.4900000E-01

BIN

0.0000000E+00

0.0000000E+00 2.2098773E-03

0.0000000E+00 7.3145528E-03 1.4974751E-03

0.0000000E+00 1.3122158E-02 4.6198099E-03 8.6212842E-04

0.0000000E+00 2.3713085E-02 1.1640342E-02 4.8346328E-03 1.6212997E-03

0.0000000E+00 4.4855360E-02 2.7792069E-02 1.6635968E-02 1.0011977E-02

3.6092025E-03

TRES 220

ROCKFLUID

RPT 1

SWT

**\$ Swkrwkrow

0 0 0.1499993

1 1 0

SLT

**\$ Slkrgkrog

0 1 0

0.5 0.3000000 0.0000000

0.52 0.2638945 0.0003750

0.54 0.2305300 0.0015000

0.56 0.1998336 0.0033750

0.58 0.1717300 0.0060000

0.6 0.1461418 0.0093750

0.62 0.1229890 0.0135000

0.64 0.1021891 0.0183750

0.66 0.0836564 0.0240000

0.68 0.0673020 0.0303750

0.7 0.0530330 0.0375000

0.72 0.0407523 0.0453750

0.74 0.0303579 0.0540000

0.74999 0.0258388 0.0585891

0.78 0.0147885 0.0735000

0.799 0.0096111 0.0838134

0.82 0.0053666 0.0960000

0.84 0.0026143 0.1083750

0.86 0.0009487 0.1215000

0.88 0.0001677 0.1353750

0.899999 0.0000000 0.1499993

**\$ Property: Rel Perm Set Num Max: 1 Min: 1

RTYPE CON 1

*MOD

1:4 1:1 1:1 = 2

RPT 2

SWT

**\$ Swkrwkrow

0 0 0.6499794

1 1 0

SLT

**\$ Slkrgkrog

0 1 0

0.12 0.2000000 0.0000000

0.14 0.1845029 0.0006551

0.16 0.1697496 0.0026203

0.18 0.1557277 0.0058957

0.2	0.1424247	0.0104812
0.22	0.1298280	0.0163769
0.24	0.1179245	0.0235828
0.26	0.1067011	0.0320988
0.28	0.0961442	0.0419249
0.3	0.0862402	0.0530612
0.32	0.0769750	0.0655077
0.34	0.0683342	0.0792643
0.36	0.0603032	0.0943311
0.38	0.0528668	0.1107080
0.4	0.0460096	0.1283951
0.42	0.0397158	0.1473923
0.44	0.0339690	0.1676997
0.46	0.0287524	0.1893172
0.48	0.0240485	0.2122449
0.5	0.0198394	0.2364827
0.52	0.0161064	0.2620307
0.54	0.0128300	0.2888889
0.56	0.0099899	0.3170572
0.58	0.0075649	0.3465357
0.6	0.0055323	0.3773243
0.62	0.0038685	0.4094230

0.64 0.0025478 0.4428319
 0.66 0.0015427 0.4775510
 0.68 0.0008230 0.5135802
 0.7 0.0003549 0.5509196
 0.72 0.0000990 0.5895692
 0.74 0.0000063 0.6295288
 0.74999 0.0000000 0.6499794

INITIAL

USER_INPUT

**\$ Property: Pressure (psi) Max: 5500 Min: 5500

PRES CON 5500

**\$ Property: Water Saturation Max: 0 Min: 0

SW CON 0

ZGLOBALC 'C7-C12' CON 5.18

ZGLOBALC 'C6' CON 1.81

ZGLOBALC 'C4+C5' CON 7.86

ZGLOBALC 'C3' CON 5.91

ZGLOBALC 'C2+CO2' CON 9.9

ZGLOBALC 'C13+' CON 1.41

ZGLOBALC 'C1+N2' CON 67.93

**\$ Property: Block Temperature (F) Max: 220 Min: 220


```

TEMPER CON      220

NUMERICAL

MAXSTEPS 9999999

DTMAX 0.1

DTMIN 0.000001

RUN

DATE 2010 1 1

**$

WELL 'Well-1'

PRODUCER 'Well-1'

OPERATE MAX STG 100000000.0 CONT

OPERATE MIN BHP 2500.0 CONT

**$      rad geofacwfrac skin

**$ UBA  ff Status Connection

**      rad geofacwfrac skin

GEOMETRY K 0.33 0.37 1.0 0.0

PERF GEOA 'Well-1'

** UBA  ff Status Connection

1 1 1 1.0 OPEN FLOW-TO 'SURFACE'

SHUTIN 'Well-1'

**$ Property: Implicit flag Max: 3 Min: 3

AIMSET CON      3

```

RESULTS SPEC 'Water Saturation'
RESULTS SPEC SPECNOTCALCVAL -99999
RESULTS SPEC REGION 'All Layers (Whole Grid)'
RESULTS SPEC REGIONTYPE 'REGION_WHOLEGRID'
RESULTS SPEC LAYERNUMB 0
RESULTS SPEC PORTYPE 1
RESULTS SPEC CON 0
RESULTS SPEC SPECKEEMOD 'YES'
RESULTS SPEC STOP

RESULTS SPEC 'Block Temperature'
RESULTS SPEC SPECNOTCALCVAL -99999
RESULTS SPEC REGION 'Layer 1 - Whole layer'
RESULTS SPEC REGIONTYPE 'REGION_LAYER'
RESULTS SPEC LAYERNUMB 1
RESULTS SPEC PORTYPE 1
RESULTS SPEC CON 220
RESULTS SPEC SPECKEEMOD 'YES'
RESULTS SPEC STOP

RESULTS SPEC 'Rel Perm Set Num'
RESULTS SPEC SPECNOTCALCVAL -99999
RESULTS SPEC REGION 'All Layers (Whole Grid)'
RESULTS SPEC REGIONTYPE 'REGION_WHOLEGRID'
RESULTS SPEC LAYERNUMB 0
RESULTS SPEC PORTYPE 1
RESULTS SPEC CON 1
RESULTS SPEC SPECKEEMOD 'YES'
RESULTS SPEC STOP

RESULTS SPEC 'Pressure'
RESULTS SPEC SPECNOTCALCVAL -99999
RESULTS SPEC REGION 'All Layers (Whole Grid)'
RESULTS SPEC REGIONTYPE 'REGION_WHOLEGRID'
RESULTS SPEC LAYERNUMB 0
RESULTS SPEC PORTYPE 1
RESULTS SPEC CON 5500
RESULTS SPEC SPECKEEMOD 'YES'
RESULTS SPEC STOP

RESULTS SPEC 'Porosity'

RESULTS SPEC SPECNOTCALCVAL -99999

RESULTS SPEC REGION 'Layer 1 - Whole layer'

RESULTS SPEC REGIONTYPE 'REGION_LAYER'

RESULTS SPEC LAYERNUMB 1

RESULTS SPEC PORTYPE 1

RESULTS SPEC CON 0.12

RESULTS SPEC SPECKEEMOD 'YES'

RESULTS SPEC STOP

RESULTS SPEC 'Permeability K'

RESULTS SPEC SPECNOTCALCVAL -99999

RESULTS SPEC REGION 'All Layers (Whole Grid)'

RESULTS SPEC REGIONTYPE 'REGION_WHOLEGRID'

RESULTS SPEC LAYERNUMB 0

RESULTS SPEC PORTYPE 1

RESULTS SPEC EQUALSI 0 1

RESULTS SPEC SPECKEEMOD 'YES'

RESULTS SPEC STOP

RESULTS SPEC 'Permeability J'
RESULTS SPEC SPECNOTCALCVAL -99999
RESULTS SPEC REGION 'All Layers (Whole Grid)'
RESULTS SPEC REGIONTYPE 'REGION_WHOLEGRID'
RESULTS SPEC LAYERNUMB 0
RESULTS SPEC PORTYPE 1
RESULTS SPEC EQUALSI 0 1
RESULTS SPEC SPECKEEMOD 'YES'
RESULTS SPEC STOP

RESULTS SPEC 'Permeability I'
RESULTS SPEC SPECNOTCALCVAL -99999
RESULTS SPEC REGION 'Layer 1 - Whole layer'
RESULTS SPEC REGIONTYPE 'REGION_LAYER'
RESULTS SPEC LAYERNUMB 1
RESULTS SPEC PORTYPE 1
RESULTS SPEC CON 100
RESULTS SPEC SPECKEEMOD 'YES'
RESULTS SPEC STOP

RESULTS SPEC 'Implicit flag'

RESULTS SPEC SPECNOTCALCVAL -99999

RESULTS SPEC REGION 'Layer 1 - Whole layer'

RESULTS SPEC REGIONTYPE 'REGION_LAYER'

RESULTS SPEC LAYERNUMB 1

RESULTS SPEC PORTYPE 1

RESULTS SPEC CON 3

RESULTS SPEC SPECKEEMOD 'YES'

RESULTS SPEC STOP

RESULTS SPEC 'Global Composition\$C' 'C1+N2'

RESULTS SPEC SPECNOTCALCVAL -99999

RESULTS SPEC REGION 'All Layers (Whole Grid)'

RESULTS SPEC REGIONTYPE 'REGION_WHOLEGRID'

RESULTS SPEC LAYERNUMB 0

RESULTS SPEC PORTYPE 1

RESULTS SPEC CON 67.93

RESULTS SPEC SPECKEEMOD 'YES'

RESULTS SPEC STOP

RESULTS SPEC 'Global Composition\$C' 'C2+CO2'
RESULTS SPEC SPECNOTCALCVAL -99999
RESULTS SPEC REGION 'All Layers (Whole Grid)'
RESULTS SPEC REGIONTYPE 'REGION_WHOLEGRID'
RESULTS SPEC LAYERNUMB 0
RESULTS SPEC PORTYPE 1
RESULTS SPEC CON 9.9
RESULTS SPEC SPECKEEMOD 'YES'
RESULTS SPEC STOP

RESULTS SPEC 'Global Composition\$C' 'C3'
RESULTS SPEC SPECNOTCALCVAL -99999
RESULTS SPEC REGION 'All Layers (Whole Grid)'
RESULTS SPEC REGIONTYPE 'REGION_WHOLEGRID'
RESULTS SPEC LAYERNUMB 0
RESULTS SPEC PORTYPE 1
RESULTS SPEC CON 5.91
RESULTS SPEC SPECKEEMOD 'YES'
RESULTS SPEC STOP

RESULTS SPEC 'Global Composition\$C' 'C4+C5'
RESULTS SPEC SPECNOTCALCVAL -99999
RESULTS SPEC REGION 'All Layers (Whole Grid)'
RESULTS SPEC REGIONTYPE 'REGION_WHOLEGRID'
RESULTS SPEC LAYERNUMB 0
RESULTS SPEC PORTYPE 1
RESULTS SPEC CON 7.86
RESULTS SPEC SPECKEEMOD 'YES'
RESULTS SPEC STOP

RESULTS SPEC 'Global Composition\$C' 'C6'
RESULTS SPEC SPECNOTCALCVAL -99999
RESULTS SPEC REGION 'All Layers (Whole Grid)'
RESULTS SPEC REGIONTYPE 'REGION_WHOLEGRID'
RESULTS SPEC LAYERNUMB 0
RESULTS SPEC PORTYPE 1
RESULTS SPEC CON 1.81
RESULTS SPEC SPECKEEMOD 'YES'
RESULTS SPEC STOP

RESULTS SPEC 'Global Composition\$C' 'C7-C12'
RESULTS SPEC SPECNOTCALCVAL -99999
RESULTS SPEC REGION 'All Layers (Whole Grid)'
RESULTS SPEC REGIONTYPE 'REGION_WHOLEGRID'
RESULTS SPEC LAYERNUMB 0
RESULTS SPEC PORTYPE 1
RESULTS SPEC CON 5.18
RESULTS SPEC SPECKEEMOD 'YES'
RESULTS SPEC STOP

RESULTS SPEC 'Global Composition\$C' 'C13+'
RESULTS SPEC SPECNOTCALCVAL -99999
RESULTS SPEC REGION 'All Layers (Whole Grid)'
RESULTS SPEC REGIONTYPE 'REGION_WHOLEGRID'
RESULTS SPEC LAYERNUMB 0
RESULTS SPEC PORTYPE 1
RESULTS SPEC CON 1.41
RESULTS SPEC SPECKEEMOD 'YES'
RESULTS SPEC STOP

RESULTS SPEC 'Grid Thickness'

RESULTS SPEC SPECNOTCALCVAL -99999

RESULTS SPEC REGION 'Layer 1 - Whole layer'

RESULTS SPEC REGIONTYPE 'REGION_LAYER'

RESULTS SPEC LAYERNUMB 1

RESULTS SPEC PORTYPE 1

RESULTS SPEC CON 70

RESULTS SPEC SPECKEEMOD 'YES'

RESULTS SPEC STOP

RESULTS SPEC 'Grid Top'

RESULTS SPEC SPECNOTCALCVAL -99999

RESULTS SPEC REGION 'Layer 1 - Whole layer'

RESULTS SPEC REGIONTYPE 'REGION_LAYER'

RESULTS SPEC LAYERNUMB 1

RESULTS SPEC PORTYPE 1

RESULTS SPEC CON 8000

RESULTS SPEC SPECKEEMOD 'YES'

RESULTS SPEC STOP